AGU PUBLICATIONS

Tectonics

RESEARCH ARTICLE
10.1002/2017TC004715

Key Points:
- The Taupo Rift evolves through asymmetric inward migration of boundary faults (width narrowing) and along-strike propagation
- Comparison between Taupo Rift and subduction and intraplate rifts suggests that the former evolves faster in particular during early stages
- Shallow voluminous magmatism aids episodic rifting. Evolution reversals (from magmatic to tectonic) also occur in subduction rifts

Supporting Information:
- Supporting Information S1

Correspondence to:
P. Villamor,
p.villamor@gns.cri.nz

Citation:
Villamor, P., Berryman, K. R., Ellis, S. M., Schreurs, G., Wallace, L. M., Leonard, G. S., … Ries, W. F. (2017). Rapid evolution of subduction-related continental intraarc rifts: The Taupo Rift, New Zealand. *Tectonics*, *36*, 2250–2272. https://doi.org/10.1002/2017TC004715

Received 3 JUL 2017
Accepted 26 SEP 2017
Accepted article online 4 OCT 2017
Published online 28 OCT 2017

Rapid Evolution of Subduction-Related Continental Intraarc Rifts: The Taupo Rift, New Zealand

P. Villamor[1], K. R. Berryman[1], S. M. Ellis[1], G. Schreurs[2], L. M. Wallace[1], G. S. Leonard[1], R. M. Langridge[1], and W. F. Ries[1]

[1]GNS Science, Lower Hutt, New Zealand, [2]Institute of Geological Sciences, University of Bern, Bern, Switzerland

Abstract The evolution of the continental intraarc Taupo Rift in the North Island, New Zealand, is rapid, significantly faster than comparative intracontinental rifts such as the African Rifts. Based on our faulting data and published geological, geophysical, and borehole data, we show that activity in the ~2 Ma Taupo Rift has rapidly and asymmetrically narrowed via inward and eastward migration of faulting (at rates of approximately 30 km Myr^{-1} and 15 km Myr^{-1}, respectively) and has propagated southward along its axis ~70 km in 350 kyr. The loci of voluminous volcanic eruptions and active faulting are correlated in time and space, suggesting that a controlling factor in the rapid rift narrowing is the presence of large shallow heterogeneities in the crust, such as large rhyolitic magma bodies generated by subduction processes, which weaken the crust and localize deformation. Eastward migration of faulting also follows the eastward migration of the volcanic arc which may be related to rollback of the Pacific crust slab at the Hikurangi subduction zone. Southward propagation of the rift is linked with southward migration of the Hikurangi Plateau/Chatham Rise subduction point and occurs episodically aided by stress changes associated with voluminous local volcanism. The large magma supply during early continental intraarc rift stages explains faster evolution (from tectonic to magmatic) than intracontinental rifts. However, the fast changes in magma supply from the subduction zone can also lead to evolution reversals (more evolved magmatic stages reverting to less evolved tectonic stages), rift cessation, and thus failed continental breakup.

1. Introduction

Rifts commonly evolve through narrowing (inward migration of boundary faults), lateral migration (of the whole rift or the rift axis), and propagation along the rift strike (Ebinger et al., 2000). These processes are often linked to an evolution from tectonic dominant to magmatic dominant with time. The narrowing and along-strike propagation modes of rift evolution have been described for several rifts worldwide including the Main Ethiopian Rift (MER)-Afar system (Agostini et al., 2011; Bonini et al., 2005; Hayward & Ebinger, 1996) (Figure 1). Lateral migration has been described for the Icelandic rift that has undergone several "jumps" to the east (Hardarson et al., 2008). In these examples, the processes underlying rift evolution are progressive crustal thinning (narrowing in the MER), translation of the ridge axis above the mantle plume (lateral migration of the Icelandic rift), and reactivation of rifting as a consequence of a change in the plate tectonic kinematics (along-strike propagation of the MER).

Rift evolution has been extensively described for large intracontinental rifts, such as the MER (e.g., Corti, 2009; Ebinger, 2005). Some of the processes described above are often characteristic of specific stages within the evolution of a rift. A typical pattern for intracontinental rift evolution, as described by Ebinger (2005), comprises three stages: birth (stage 1 or initiation), adolescence (stage 2 or intermediate), and maturity (stage 3 or continent breakup). In the initiation stage of a rift, extensional faulting and cracking develops in cold, strong, and thick continental crust, commonly forming an asymmetric graben, and often along existing planes of weakness in the crust. As displacement accumulates along the rift-bounding active faults, they also propagate along strike linking with other faults and forming long rift segments. At the same time, the crust begins to thin, and magmatism from the mantle or deep crustal levels may appear along, or in association with, faults. As the rift evolves into the intermediate stage, thinning of the lithosphere is more pronounced; magmatism from shallower crustal levels and new faulting appears in the central part of the rift (early stages of the narrowing process mentioned above) as displacement also continues to accumulate on the border faults. In the breakup stage, melt rises to shallower levels, localizing faulting in the central part, and rift narrowing is most intense. At this stage, strain is mainly accommodated by dike intrusion along the rift axis with lesser seismogenic faulting, and border faults become inactive.

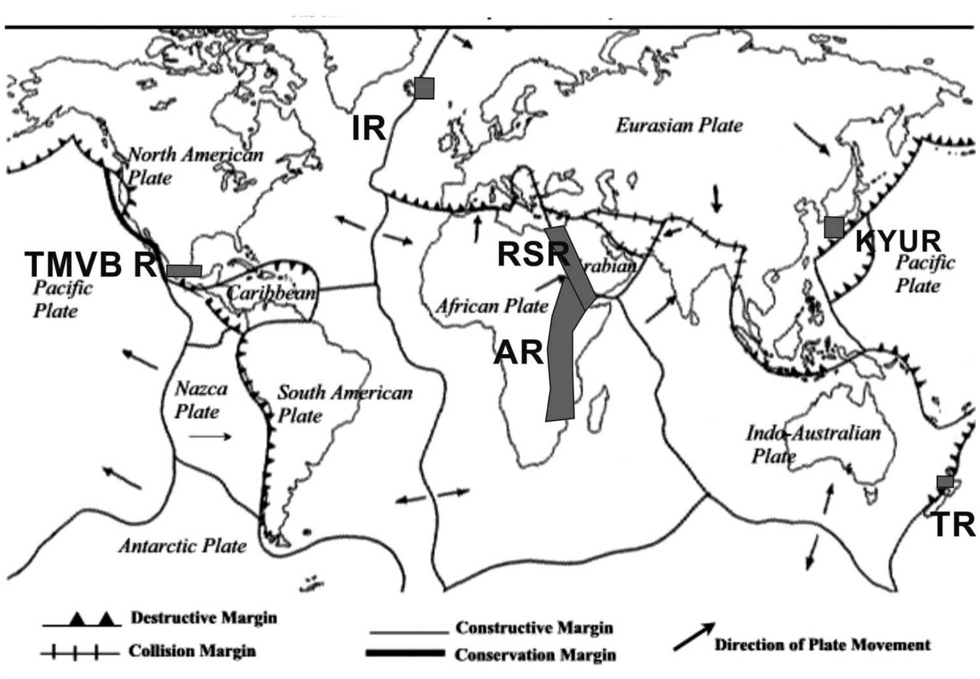

Figure 1. Locations of continental rifts discussed in this study with reference to the tectonic plates. AR, African Rift (including south to north the rifts of Tanzania Kenya, Mid-African Rift, and Afar); IR, Icelandic Rift; KYUR, rifts in Kyushu Island; RSR, Red Sea Rift (including from north to south Suez and Red Sea Rifts); TMVB R, Trans-Mexican Volcanic Belt Rift; and TR, Taupo Rift.

Most studies of continental rift evolution have focused on intracontinental (intraplate) rifts (e.g., MER) and rifts associated with mid-ocean ridges (e.g., Iceland). Here we introduce the evolution of continental intraarc rifts (a rift associated with active volcanism and upper plate extension of a subduction zone) into the literature on rift evolution with emphasis on the characterization of the 2-million-year-old Taupo Rift (Figure 2), New Zealand. The Taupo Rift is an ideal natural laboratory for gaining insights into the rift evolution because of its youth, and high rates of tectonic and volcanic processes. We also explore evolution of other continental intraarc rifts such as Kyushu, Japan, and the Trans-Mexican Volcanic Belt.

The Taupo Rift (37°30′S to 39°30′S latitude; Figures 1–3) formed in continental crust in association with continued subduction of the Pacific Plate beneath the Australian Plate in the North Island, New Zealand, and is the southern continuation of the Havre Trough back-arc basin (Figure 2a) (Parson & Wright, 1996). Extension in the Taupo Rift coincides with the Hikurangi subduction zone's volcanic arc (i.e., the Taupo Volcanic Zone (TVZ); Figure 2a) and is thus referred to as an intraarc rift.

The TVZ can be divided into three geographic sections based on the distribution of volcanism (Figure 3) (Wilson & Rowland, 2016): (1) the northern TVZ (north of Okataina Volcanic Center (OVC); Figure 2b) is dominated by andesitic and dacitic volcanism; (2) the central TVZ is characterized by voluminous, dominantly rhyolitic volcanism (between the Taupo Volcanic Center (TVC) and the OVC; Figure 2b); and (3) the southern TVZ (south of the TVC; Figure 2b) mainly comprises composite andesitic-dacitic cone volcanoes. The Taupo Rift is known for its high heat flow (present-day average heat flow of 700 mW/m^2; Bibby et al., 1995) and for hosting four supereruptions (with individual volumes $>$500 km^3; Wilson et al., 2009). Extension rates derived from contemporary geodetic (Wallace et al., 2004) and Quaternary fault data (Villamor & Berryman, 2001, 2006a; Lamarche et al., 2006) increase northward from 2–4 mm/yr at the southern termination of the Taupo Rift to 10–15 mm/yr at the Bay of Plenty coast (Figure 2b).

We synthesize published and new (active faulting) geological data on the locus and extent of faulting along with a summary of published stratigraphic (including borehole data) and geophysical (gravity, seismic reflection, and resistivity) data to construct the evolutionary history of the rift. Numerous datable geomorphic surfaces and volcanic derived deposits (supporting information) (Leonard et al., 2010) enable an unusually detailed analysis of the evolution of faulting in the Taupo Rift.

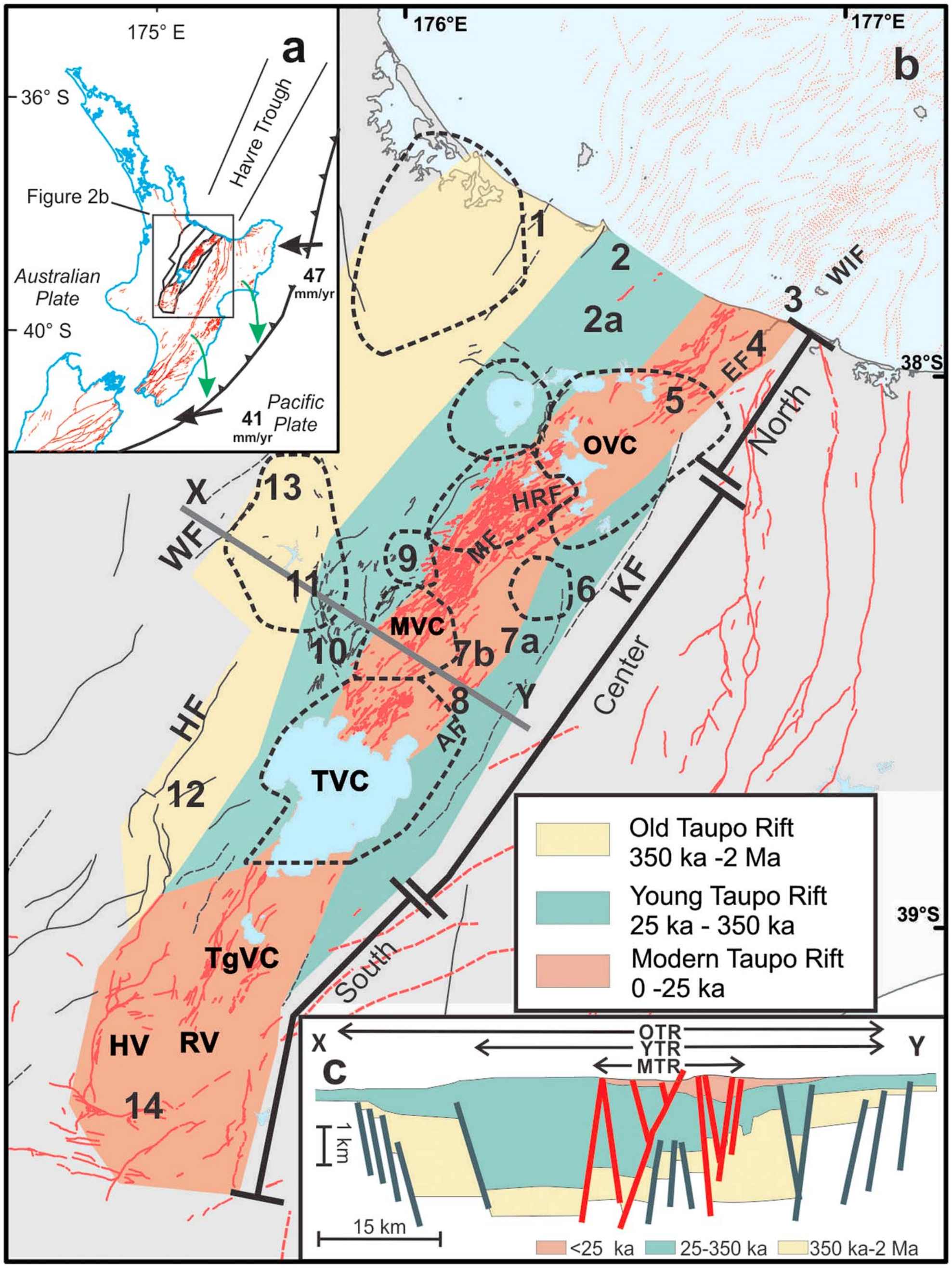

Figure 2. (a) Plate tectonic setting of the Taupo Rift. Black arrows indicate the relative plate motions. Green arrows indicate the current fore-arc rotation. (b) Evolutionary stages of active faulting in the Taupo Rift: modern Taupo Rift (MTR; 0–25 ka), young Taupo Rift (YTR; 25–350 ka), and old Taupo Rift (OTR; 350 ka–2 Ma). Dashed red lines offshore are the active faults (Lamarche et al., 2006). Red lines onshore are the active faults (bold lines are the faults clearly mapped from aerial photography analysis, and dashed lines are the faults inferred from geophysical investigations or topographic lineaments). Black lines are the inactive faults (bold lines are the faults mapped at the surface, and dashed lines are the faults inferred from geophysical investigations or topographic lineaments). Volcanic centers are OVC: Okataina Volcanic Center, MVC: Maroa Volcanic Center, TVC: Taupo Volcanic Center, RV: Ruapehu Volcanic Center, TgVC: Tongariro Volcanic Center, HV: Hauhungatahi Volcano. Faults are AF: Aratiatia Fault, EF: Edgecumbe Fault, HF: Hauhungaroa Fault, HRF: Highlands Road Fault, KF: Kaingaroa Fault MF: Maleme Fault, WF: Waipapa Fault, WIF: White Island Fault. See text for details on fault initiation and cessation for map locations 1 to 14. (c) Schematic cross section (*x*-*y*) showing relationships between basin infill and fault migration. Location of section is shown in Figure 2b.

We show that the Taupo Rift displays all three modes of evolution, for example, narrowing, lateral migration, and along-strike propagation, similar to intracontinental rifts, and suggest possible mechanisms and processes responsible for these evolution modes. We also compare styles and rates of evolution with other rifts and explore if the three stages of evolution defined by Ebinger (2005) and Corti (2009) can be found in the Taupo Rift.

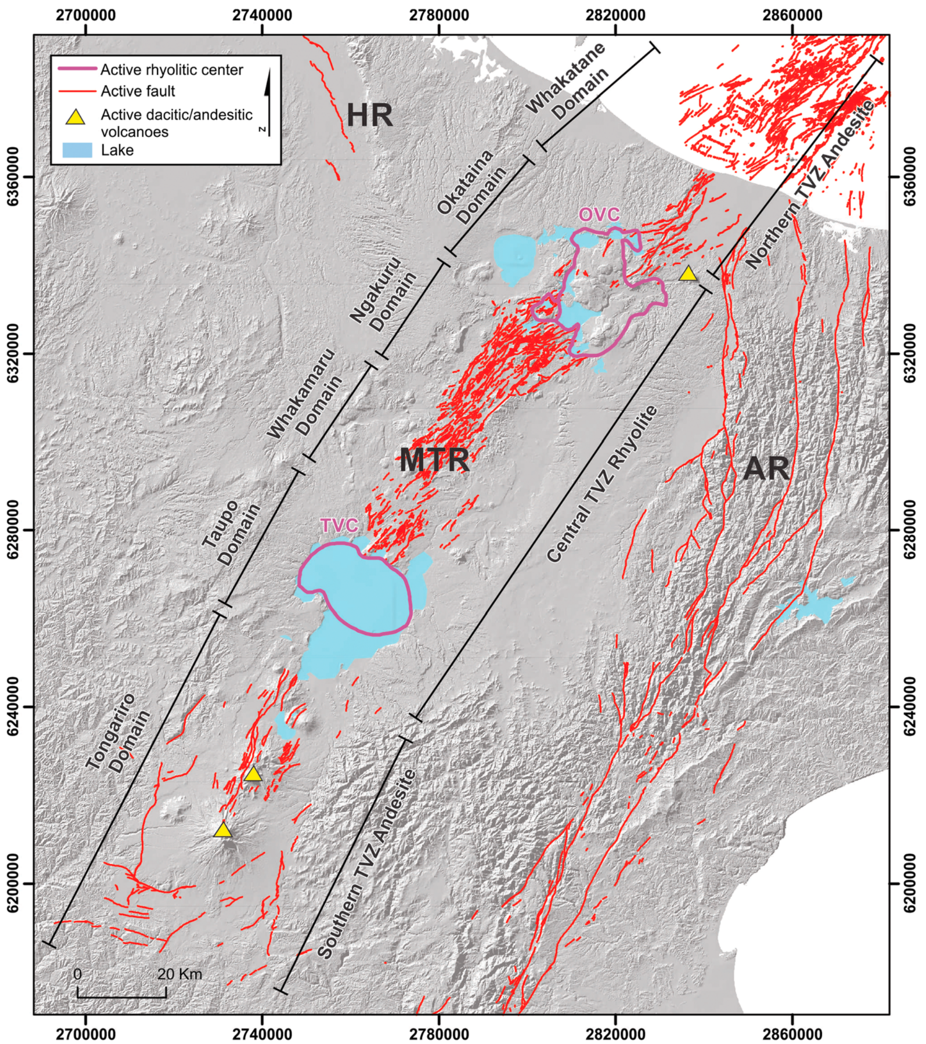

Figure 3. Active faults (red lines) of the modern Taupo Rift (MTR) and surroundings (AR, Axial Ranges; HR, Hauraki Rift). Tectonic domains or segments of the MTR are from Rowland and Sibson (2001) (labeled on the left side of the rift). Volcanic domains by Wilson et al. (1995) (labeled on the right side of the rift), with TVZ = Taupo Volcanic Zone. Onshore active faults from New Zealand active fault database (http://data.gns.cri.nz/af/). Offshore faults are from Lamarche et al. (2006).

2. Evidence for the Evolution of the Taupo Rift

2.1. Rift Evolution Illustrated by Surface Faulting Data

The onshore history of active faulting in the Taupo Rift can be divided into three stages (Villamor & Berryman, 2006b): the old Taupo Rift (2 Ma–350 ka), the young Taupo Rift (350–25 ka), and the modern Taupo Rift (25–0 ka) (Figures 2b and 2c), based on the surface expression of fault activity. This nomenclature parallels that assigned to different evolutionary stages of volcanism in the TVZ (old TVZ from 2 Ma, young TVZ from 350 ka, and modern TVZ from 61 ka; Wilson et al., 1995) but with slightly different time bounds chosen to maximize constraints on faulting activity. The evolution of faulting presented here pertains primarily to the onshore part of the rift.

Temporal constraints on fault activity along the rift are not homogeneous because the volcanic deposits, which provide the time horizons for evaluating fault activity, vary across and along the rift (Figure S1 and Tables S1 and S2 in the supporting information). Also, rapid long-term subsidence in some areas (3–7 mm/yr for the late Pleistocene) (Chambefort et al., 2014; Downs et al., 2014; Mouslopoulou et al., 2008; Villamor & Berryman, 2006a, 2006b) and extensive and thick ignimbrite sheets and pyroclastic deposits from eruptions at about 550 ka and at 350–240 ka (>3000 km^3; Leonard et al., 2010) have buried the record of faulting older than about 350 ka in many places. For these reasons, the exact onset of extensional faulting, as well as the pattern of early stage faulting within the Taupo Rift, is uncertain, although borehole information is starting to provide some information (see below). Initiation of the extensional regime can be defined as coeval with initiation of TVZ volcanism at ~2 Ma (Wilson et al., 2009; Cole & Spinks, 2012; Chambefort et al., 2014). Faulting could have initiated somewhat later (post-1.5 Ma) as suggested by changes in the tectonic regime from strike slip to extension, inferred from structural interpretations of geothermal borehole stratigraphy at Kawerau (location 5 in Figure 2b and Text S1 in the supporting information) (Milicich, Wilson, Bignall, Pezaro, & Bardsley, 2013).

We describe next the three stages of the Taupo Rift evolution from surface faulting data. Detailed explanations for information compiled at different locations along the rift are presented in Text S1.

2.1.1. The Old Taupo Rift

In the old Taupo Rift (Figure 2b) faults were active after ~2–1.5 Ma and before ~350 ka (although in some locations activity continued to ~230 ka). Three locations on the western margin of the old rift show that faulting migrated toward the center of the rift between ~350 and 230 ka and the rift narrowed by 20 km (locations 1, 12, and 13 in Figure 2b and Text S1).

Two rift-bounding faults, the Waipapa (location 13 in Figure 2b and Text S1) and the Hauhungaroa (location 12 in Figure 2b and Text S1) Faults, displace ~1.21–1.68 Ma old ignimbrites, whereas the extensive ~350 ka ignimbritic deposits that form most of the landscape overlie the faults without displacement (geomorphic analysis for this study) (Blank, 1965; Leonard et al., 2010). At location 1 (Figure 2a and Text S1), basalts and dacites of 2.5–2.9 Ma age (Briggs et al., 2005) are displaced by faults with predominant NE trends (Figure 4a), but the extensive ~240 ka old ignimbrite constructional surface is not displaced by these faults.

While there is a clear eastward shift of fault activity on the western side, the eastern boundary of the old Taupo Rift (the offshore White Island Fault and the onshore Edgecumbe and Kaingaroa Faults; WIF, EF, and KF in Figure 2b) has been active at least until ~230 ka (e.g., WIF and EF are still active; see discussion on faults below), suggesting that the eastern boundary of the old and young Taupo rifts coincide.

2.1.2. The Young Taupo Rift

Faults within an ~50 km wide zone that we define as the young Taupo Rift show clear activity in the period between ~350–230 ka and ~25 ka. Note that the primary products of the Oruanui eruption, dated at 25.4 ka (Vandergoes et al., 2013), are not displaced by the young Taupo Rift, and thus, a better date for the lowest time bound of the activity would be 25.4 ka. We have used the time bound of 25 ka for simplicity.

Along the western margin of the northern and central sectors of the young rift, faults were active post-350 ka but activity ceased prior to or at about 25 ka, showing a further shift in fault activity to the modern Taupo Rift. For example, in the area to the NNW of the Okataina Volcanic Center (location 2a in Figure 2b and Text S1), aerial photo review shows that ~61–45 ka old ignimbrites (Nairn, 2002; Wilson et al., 2007) and younger alluvial terraces that are incised in the ignimbrite constructional surface are not displaced by faults. Moreover, ~322–240 ka old formations exposed in the coastal cliffs at Maketu (location 2 in Figure 2b (Manning, 1995; Briggs et al., 2005; Briggs et al., 2006) and Text S1) are offset by several normal faults (Figures 4b and 4c and Table S3), but the overlying 240 ka old ignimbrites and the Last Interglacial (~125 ka) paleosol are not displaced, indicating that faulting had ceased before 240 ka.

Cessation of faulting before approximately 25 ka associated with eastward migration of the young Taupo Rift western boundary is also clear farther south. In the central sector of the young Taupo Rift, the north trending Pokuru Fault displaces ~140–250 ka old volcanic domes of the Maroa Volcanic Center (location 10 in Figure 2b) but does not displace the 25.4 ka old Oruanui formation (age from Vandergoes et al., 2013) or younger deposits exposed in trenches (Text S1 and Figure S3). Nearby, NNW trending fault scarps of the Thorpe Road Fault displace the ~240 ka old deposits but paleoseismic trenches show that younger deposits $<$30 ka in age are not displaced (location 9 in Figure 2b, Figures 5 and S4, and Table S4) (Leonard, 2003; this study).

Again, migration of the eastern margin of the young Taupo Rift is not as clear as for the western margin (Figure 2b). In the northern sector the old, young, and modern rift boundaries almost coincide. Immediately offshore of the northern sector, Taylor et al. (2004) showed that the White Island Fault (location 3 in Figure 2b and Text S1) has remained the boundary of the rift since 1 Ma ago. In the central sector,

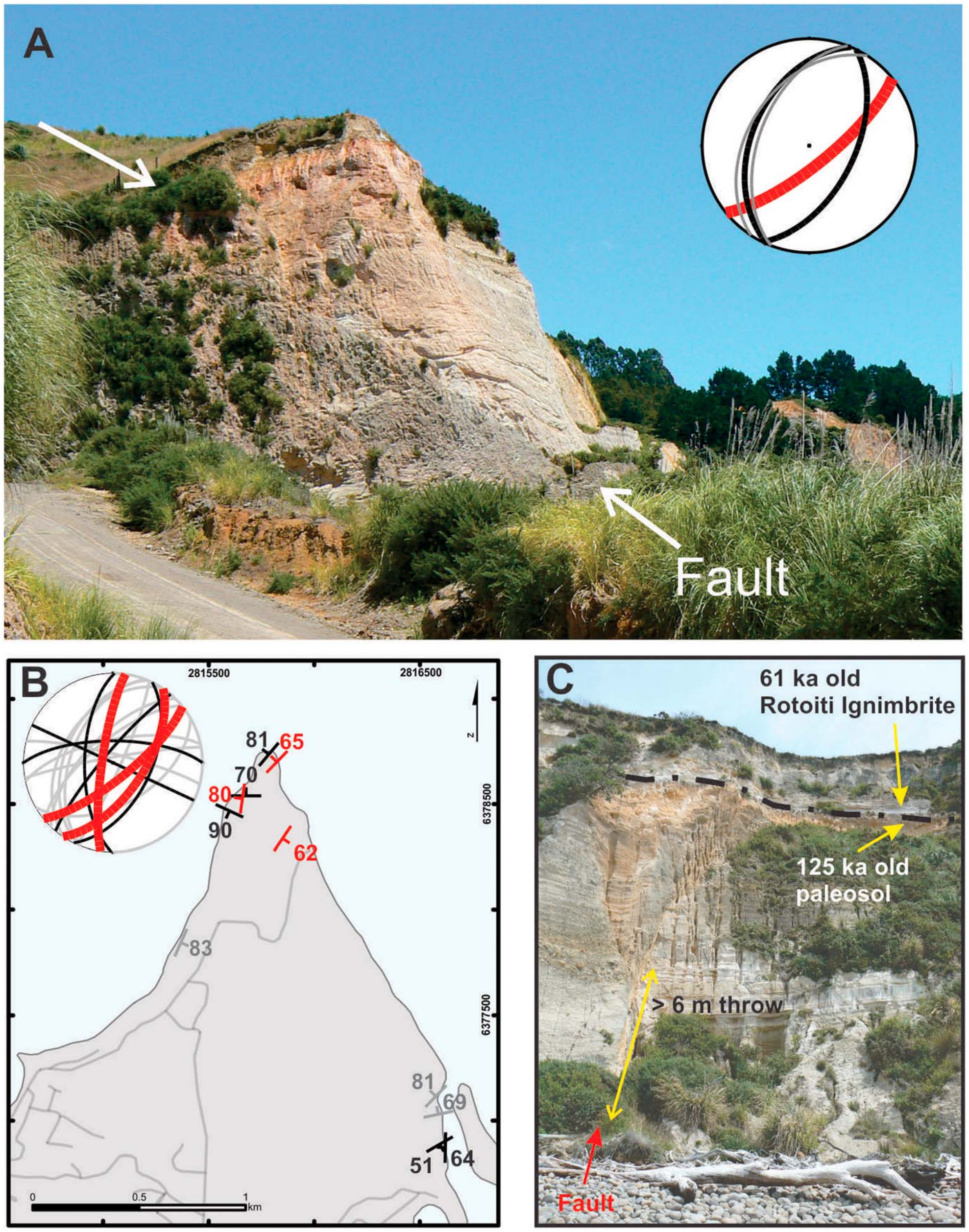

Figure 4. (a) Western boundary fault of the old Taupo Rift (location 1 in Figure 2b) displacing >2 Ma old basalt and dacites (ages from Briggs et al. (2005)). Strike of faults in the area is similar to the active faults in the Taupo Rift (i.e., NE-SW). (b) Western boundary faults of the young Taupo Rift at Maketu horst (location 2 in Figure 2b). Fault strikes from major faults (red major planes) are in agreement with the general NNE-SSW to NE-SW strike of faults in the Taupo Rift. Faults are steeply dipping, with dips to east and west. (c) Several normal faults within the Maketu horst/elevation are exposed in the coastal cliffs, where they offset alluvial and volcanic deposits, dated between the Matahina (~320 ka) and the Mamaku Plateau (240 ka) formations, by >6 m. The Mamaku Plateau formation (based on aerial photo analysis) and the Last Interglacial (~125 ka) paleosol (exposed in cliffs) are not displaced. The fault history seen at Maketu suggests that extension in the old Taupo Rift to north of Okataina Volcanic Center was active for some time after 320 ka (Matahina Ignimbrite eruption), but had largely ceased before the Mamaku Ignimbrite eruption from Rotorua caldera at 230 ka. No extension has occurred onshore after the ~125 ka Last Interglacial. In the stereographic projections (lower hemisphere), red great circles are the faults with displacements larger than 10 m, black great circles are the faults with displacements from 10 to 1 m, and grey great circles are the faults with displacements less than 1 m. See Table S3 for the fault data.

rift-bounding faults migrated 5 to 12 km westward some time since ~230 ka (migration from location 6 to location 7b) as illustrated by the displacement of the ~350 ka old deposits by the Kaingaroa Fault (location 6 in Figure 2b and Text S1) (Leonard et al., 2010), but with no evidence of displacement of the ~230 ka old ignimbrite sheets (this study; Downs et al., 2014).

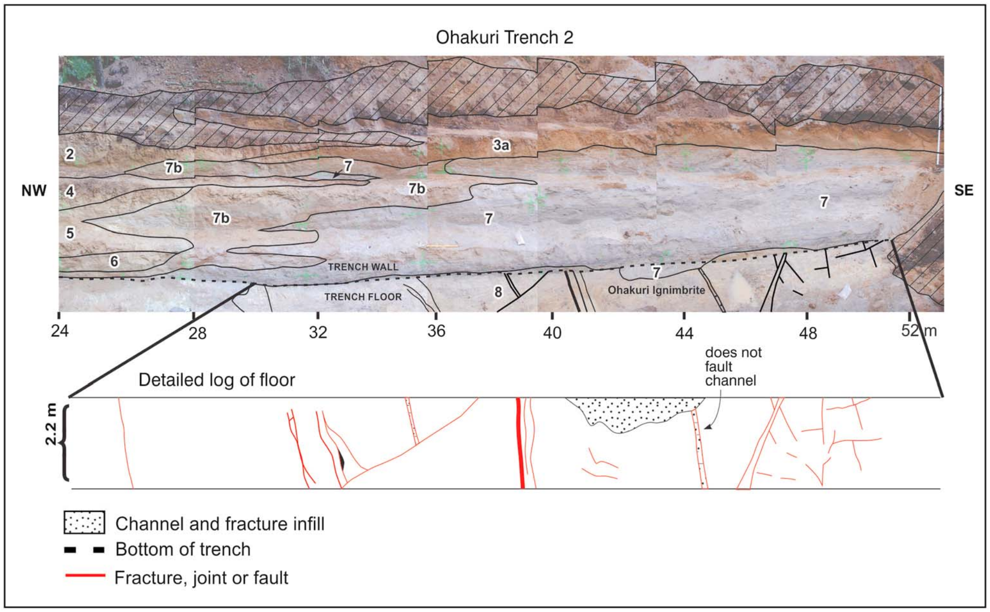

Figure 5. Thorpe Road Fault (location 9 in Figure 2b). Photomosaic of trench Ohakuri #2 and trench log (for the trench location and a more detailed figure, see Figure S4 and Table S4). The trench was excavated in a valley incised into Ohakuri Ignimbrite. The trench shows <28,000 year old nondisplaced units (units 1 to 7 exposed on the trench wall; descriptions in Table S4) overlying fractured and faulted Ohakuri Ignimbrite (unit 8 exposed on the trench floor). Tephras provide the age of sediments and thus timing of faulting (see Table S4). The ~13,600 year old Waiohau tephra was present in the trench (base of unit 4). The ~30,000 year old Okaia tephra was not present in the trench but found at an exposure 50 m away from the trench, and Okaia tephra could be correlated to unit 7 in the trench. The section of the trench log shown is from meter 24 to 52 of the full trench length. Horizontal and vertical scales are the same. Bottom of the figure shows the detail of the log of the trench floor (from meter 30 to 52), showing orientation and characteristics of fracturing and faulting of Ohakuri formation.

At approximately the same time as active faulting migrated inward to the young Taupo Rift (<350 ka), the southernmost sector of the rift was established (location 14 in Figure 2b) (Villamor & Berryman, 2006b). While some faults may have already been active by 400 ka in the southern sector, most of the rift-related fault activity in the south initiated after 350 ka, coincident with supereruptions occurring in the central sector (Villamor & Berryman, 2006b).

2.1.3. The Modern Taupo Rift

Fault activity has focused within the modern Taupo Rift from ~25 ka to the present. The modern active rift is a narrow fault belt, ranging in width from 15 km in the northern sector to 40 km in the southern sector (Figures 2b and 3). Normal faults are closely spaced across the rift, with surface trace spacing ranging from <100 m to approximately 3 km in the central rhyolitic sector (Rowland & Sibson, 2001; Villamor & Berryman, 2001; Seebeck, Nicol, Villamor, et al., 2014) and the northern sector (Begg & Mouslopoulou, 2010; Lamarche et al., 2006). Fault spacing increases to approximately 5 to 10 km in the southern, andesite-dominated sector (Villamor & Berryman, 2006a). The rift is partitioned along strike into rift segments that are 20 to 40 km long (Rowland & Sibson, 2001) (Figure 3). Normal fault trends range from N20°E in the southernmost sector to N45°E in the central and northern sectors (Acocella et al., 2003; Lamarche et al., 2006; Rowland & Sibson, 2001). At its southern end, the rift terminates abruptly at active faults with a predominantly normal displacement, striking at high angles (N65°E) to the marginal NNE trending faults of the rift (Villamor & Berryman, 2006a; Gómez-Vasconcelos et al., 2016). Active faults from Okataina Volcanic Center (OVC in Figure 2b) southward to the Taupo Volcanic Center (TVC) alternate along strike with active, rhyolite-dominant volcanic centers. Volcanoes are located along the axis of the rift in the southern andesite-dominant sector (the Tongariro Domain of Rowland and Sibson (2001)). North of the Okataina Volcanic Center, in the northern sector of the rift and offshore, volcanoes are located near to the eastern boundary of the rift (Nairn, 2002).

Fault activity in the modern Taupo Rift is evidenced by clear displacements of the 18–25 ka and younger geomorphic surfaces (Figure 6). These include the approximately 18 ka old lahar surfaces around the southernmost andesitic volcanoes (Lee et al., 2010; Townsend et al., 2008), the approximately 15–25 ka old alluvial terraces incised into older ignimbrites and domes around Okataina Volcanic Center (Nairn, 2002), and the old

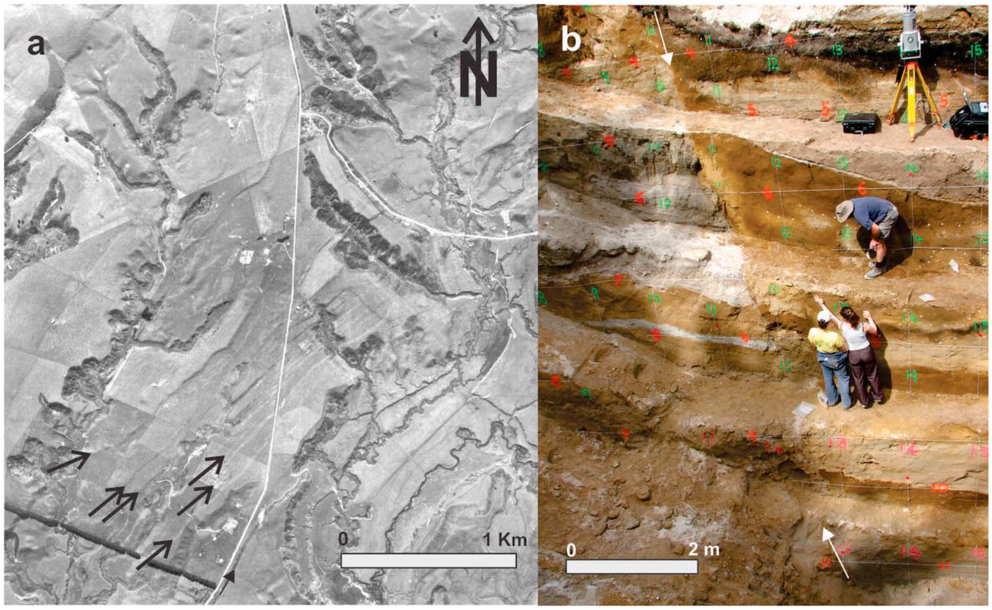

Figure 6. Example of active faulting within the modern Taupo Rift. (a) Active fault scarps of the Maleme Fault Zone (rift axis; Villamor & Berryman, 2001) observed in the 1960s aerial photographs (1:16,000 scale, NZ Aerial Mapping). Note that some fault scarps are marked with black arrows. Faults are displacing <25 kyr old surfaces. See Figure 2 for the location of the Maleme Fault Zone. (b) Example of current fault activity in a paleoseismic trench with the modern Taupo Rift (Foster trench, Highlands Road Fault, unpublished). Fault plane is marked with white arrows. The sediments in the trench are mainly volcanic air fall deposits with some alluvial layers at the base with ages from ~40 ka to 2 ka. The youngest tephra from Taupo formation (Table S1) is displaced. See Figure 2 for the location of the Highlands Road Fault.

constructional surface from the large rhyolitic Oruanui eruption at 25.4 ka (age from Vandergoes et al. (2013)) and their derived alluvial and lacustrine deposits (Manville & Wilson, 2004) in the central sector. Continuing activity on these faults is indicated by the location of shallow seismicity (e.g., Bryan et al., 1999), geodetic evidence for high strain rates (Wallace et al., 2004), historic fault surface rupture (1987 Edgecumbe earthquake; Beanland et al., 1989), geomorphic and paleoseismic evidence (Figure 6) (e.g., Begg & Mouslopoulou, 2010; Nairn, 2002; Nicol et al., 2009; Villamor et al., 2011; Villamor & Berryman, 2006a), and offshore seismic reflection studies close to the coast (Lamarche et al., 2006).

2.2. Subsurface Indicators of Rift Evolution From Geophysical and Geological Data

Based on gravity Bouguer anomalies (Figure S2) (Stagpoole & Bibby, 1999), the width of the old Taupo Rift is ~70 km, coincident with the major NE trending gravity anomaly in the region (Seebeck, Nicol, Villamor, et al., 2014; Wilson & Rowland, 2016). We interpret the steep gravity contours at the margins of the anomaly as displacement along the older rift-bounding faults that are now buried by <350 ka deposits. On the east side, the anomaly is large (+20 mGal) and the contours defining the rift margin are very straight and continuous along the rift. On the west side, the anomaly is smaller and the contours step left laterally with sharp NW trending accommodation zones. This gravity anomaly coincides with mapped faults to the south (Waipapa Fault; Figure 2b) and with a sharp subrectilinear contact between Pliocene and Pleistocene volcanic formations to the north (Leonard et al., 2010). Larger gravity anomalies within the rift are associated with large extinct and active calderas (see discussion in Wilson & Rowland (2016)).

Quantifying crustal thinning and stretching in the Taupo Rift is difficult, because it exhibits a heterogeneous crustal structure that reflects a complex evolution with superposition of different crustal processes such as faulting, intrusion, and volcanism (Bannister et al., 2013, 2015; Hurst et al., 2016; Wilson & Rowland, 2016). In the central sector (rhyolite sector of the TVZ), the Moho lies at ~25–30 km depth over the width of the old Taupo Rift (Bannister et al., 2004; Harrison & White, 2004; Stern & Benson, 2011). In the axial part of the rift (approximately the width of the modern Taupo Rift), a strong contrast in velocity at 16 km depth seems to coincide with a transition to heavily intruded crust (Bannister et al., 2004; Harrison & White, 2004; Stern & Benson, 2011). Such underplating can explain the relatively flat, deep Moho derived from seismic velocities, despite crustal stretching by at least 10 km (Nicol & Wallace, 2007). Assuming that the original greywacke crust of the rift was approximately 30 km thick (Horspool et al., 2006), this means that the greywacke crust of the central Taupo rift has thinned by approximately 14 km, an amount that is compatible with stretching 30 km thick crust by 10 km over the width of the modern Taupo Rift (20 km). Crustal studies are not so exhaustive in the southern TVZ, but the existing literature points to a thicker, greywacke-dominated crust in the south (~40 km, south of Tongariro Volcanic Center) and anomalously deep seismicity (down to 20 km beneath Ruapehu and to 40 km further south) (Reyners et al., 2007). The thicker crust in the southern TVZ compared to the central TVZ suggests a less evolved rift to the south.

Magnetotelluric studies show large areas of partial melt below 10 km (Heise et al., 2010). The brittle-ductile transition in this axial region is approximately 6–8 km deep (Bryan et al., 1999), but 3-D V_p, V_p/V_s, Q_p, and Q_s volumes show a high level of heterogeneity at a range of length scales in the midcrust near the roots of active geothermal systems (Bannister et al., 2013). This suggests brittle-ductile processes transitioning at a range of depths in association with plutonic bodies (Bannister et al., 2013; Heise et al., 2010; Sherburn et al., 2003), which together with geothermal circulation causes high heat flow there (Bibby et al., 1995; Wilson & Rowland, 2016). Such high heat flow along with variable depth to the brittle-ductile transition may promote localization and inward migration of rift faulting through time (e.g., Kissling & Ellis, 2011).

Shallow subsurface studies also support inward fault migration over time. On the western margin of the young rift, large fault throws in post-350 ka deposits have been proposed based on resistivity data (Bibby et al., 2008) (location 11 in Figure 2b and Text S1), suggesting extensive faulting between 350 ka and 25–18 ka. Likewise, large displacements of ~350 ka old deposits sealed by ~230 ka old deposits have been interpreted on the eastern side based on seismic reflection and gravity data (Stagpoole, 1994) (location 6 in Figure 2b and Text S1). Near the eastern boundary of the modern rift, borehole data at the Ohaaki geothermal field show clear faulting in pre-350 ka deposits (location 7a in Figure 2b) and some intra-350 ka deposits, but no faulting after ~280 ka (Milicich et al., 2010; Mroczek et al., 2016). Finally, in the Kawerau geothermal field (location 5), an approximately 2 km inward fault migration from the old to the modern rift boundary can be inferred from interpretation of timing and location of faulting in boreholes (Milicich, Wilson, Bignall, Pezaro, Charlier, et al., 2013) and aerial photo reviews (this study).

Subsurface data can be used to track fault slip rates though time and show that central rift faults have faster slip rates in modern times than when averaged over a longer time frame when a broader rift accommodated the regional extension. For example, slip rates on the White Island Fault and the Edgecumbe Fault (from seismic reflection data; locations 3 and 4 in Figure 2b and Text S1) have increased during the last 300 kyr (Mouslopoulou et al., 2008; Taylor et al., 2004). This suggests that, given a constant regional extension for the rift for the last 1.5 Ma (Nicol & Wallace, 2007), prior to 300 ka, the deformation was distributed across a wider zone, but in more recent times, fewer faults with faster slip rates have accommodated the regional extension.

At the Kawerau geothermal field (location 5 in Figure 2b and Text S1), Milicich, Wilson, Bignall, Pezaro, Charlier, et al. (2013) documented a progressive increase in subsidence rates over the last 50 ka, which may be due to increasing fault slip rates. In the Ngatamariki geothermal field (location 7b in Figure 2b and Text S1), similar fault throw values of post- and pre-350 ka markers suggest initiation of faulting or an increase in fault slip rates after 350 ka (Arehart et al., 2002; Chambefort et al., 2014). At the Rotokawa geothermal field (location 8 in Figure 2b and Text S1), comparison of total fault throw of the top of basement and the ~350 ka ignimbrites (McNamara et al., 2016) and the recent slip rate on the Aratiatia Fault (Litchfield et al., 2014) suggests that fault activity close to the young Taupo Rift boundary increased after 350 ka. Thus, geothermal field data show evidence for increasing fault slip rates with time, suggesting that fewer, more central, faults are taking up the regional extension.

2.3. Evolution of Volcanism as an Indicator of Rift Evolution

A possible spatial and temporal association between magmatism and faulting is suggested by the geographical coincidence of current active faulting (modern Taupo Rift; Figure 2) and rhyolitic volcanism (OVC, TVC, and RV; Figure 2b) in a narrow band. Wilson et al. (1995) proposed a temporal and spatial evolution of volcanism in the TVZ where volcanism has occupied the whole length of the rift but has progressively occurred in a narrow zone. They define three stages, old, young, and modern TVZ with the following respective time frames: ~2 Ma to 350 ka, 350 to 61 ka, and 61 ka to present (see updated model in Wilson & Rowland (2016)).

The time frames for the evolution of volcanism (TVZ) and active faulting (Taupo Rift) are similar, but not precisely the same. For example, the modern TVZ has slightly different initiation time than the modern Taupo Rift (61 and 25 ka, respectively). Both show a tendency for narrowing in their spatial distribution with time. However, one difference is the presence of volcanism (a small andesitic volcanic cone; Hauhungatahi Volcano; Figure 2b) in the southern sector at ~1 Ma (e.g., Wilson & Rowland, 2016), suggesting that volcanism was present before NE trending faulting initiated at ~350 ka in this region (Villamor & Berryman, 2006b).

Andesitic units occur above basement rocks from at least 2 Ma (Wilson et al., 2009) and below the massive post-1.6 Ma rhyolitic deposits in boreholes in geothermal fields in the central and northern sectors of the TVZ (see compilation in Wilson & Rowland (2016)). The southern sector of the TVZ is mainly andesitic and lacks rhyolitic volcanism (e.g., Gamble et al., 2003). These observations led Price et al. (2005) to suggest that andesitic volcanism precedes rhyolitic volcanism and that the southern sector is currently at an early stage of volcanic evolution. The largest volume of volcanic rocks in the southern sector postdates 300 ka (Gamble et al., 2003).

To explore whether there is a spatial and temporal correlation between main rhyolitic volcanic centers and the migration of faulting described above, we have overlain the rhyolitic centers that were active during the different faulting stages on time-bound fault maps (Figure 7). Rhyolitic volcanism started in the TVZ around 1.6 Ma and underwent two periods of large voluminous volcanism, one peaking at around 1 Ma and a larger one between 350 and 230 ka (Houghton et al., 1995; Leonard et al., 2010; Wilson et al., 2009). The second period produced at least 6000 km^3 of rhyolite in several caldera eruptions, including one super-eruption. The volcanic products of this period obscure tectonic and volcanic information of the rift, and thus, we are not able to evaluate rift changes associated with the 1 Ma old phase.

In Figure 7, we present the stages defined by the faulting history and coeval rhyolitic volcanism. To highlight the timing of voluminous rhyolitic volcanism (350–230 ka), we have divided the evolution of the old Taupo Rift into two intervals. Prior to 350 ka, both the rhyolitic volcanism (Leonard et al., 2010) and faulting (this study) were more widespread across the width of the rift than post-230 ka (Figure 7), suggesting a possible temporal and spatial association.

3. Discussion

3.1. Spatial and Temporal Evolution of the Taupo Rift

With the information compiled above we propose an evolution of the Taupo Rift (updated and refined from Villamor & Berryman (2006b)), in which the locus of fault and volcanic activity has migrated inward, slightly eastward, and propagated southward, in three stages (Figure 8). In stage I, the faults occupied the central and northern sectors of the TVZ with rhyolitic volcanism distributed in the whole rift width. In stage II, the western border fault migrated inward (fault a to fault c) and the rift propagated south (generation of faults f, g, h, and i). Rhyolitic volcanism had also localized in a narrower zone in the central and northern sectors, and andesitic volcanism initiated (or intensified) in the south. In stage 3, both border faults of the central and northern sectors further migrated inward (to faults d and e) as rhyolitic volcanism also further localized into the currently active centers.

Timing of evolution of faulting and rhyolitic volcanism seem to coincide in general terms but there are some differences mentioned above. Here we propose a simplified model and it is likely that, at different latitudes, the rift may have evolved with slightly different temporal stages. For example, the chronology of the last stage could have been slightly different around Okataina and Taupo Volcanic Centers. In the former, large caldera forming ignimbritic eruptions occur around 61 ka (the modern TVZ of Wilson et al. (1995)), while in the latter they occurred around 25 ka. Because surficial chronological markers are not homogenously distributed along the rift, refinement of this timing will have to come from new borehole data.

An important temporal association is the occurrence of the 350-230 ignimbrite flare-up (Houghton et al., 1995) with clear narrowing of faulting and a sudden along-strike propagation of the rift (stage I to stage II). An increase in the andesitic volcanism in the southern end of the TVZ occurs around the time of active fault propagation (Tongariro and Raupehu Volcanic Centers are younger than ~300 ka; Gamble et al., 2003).

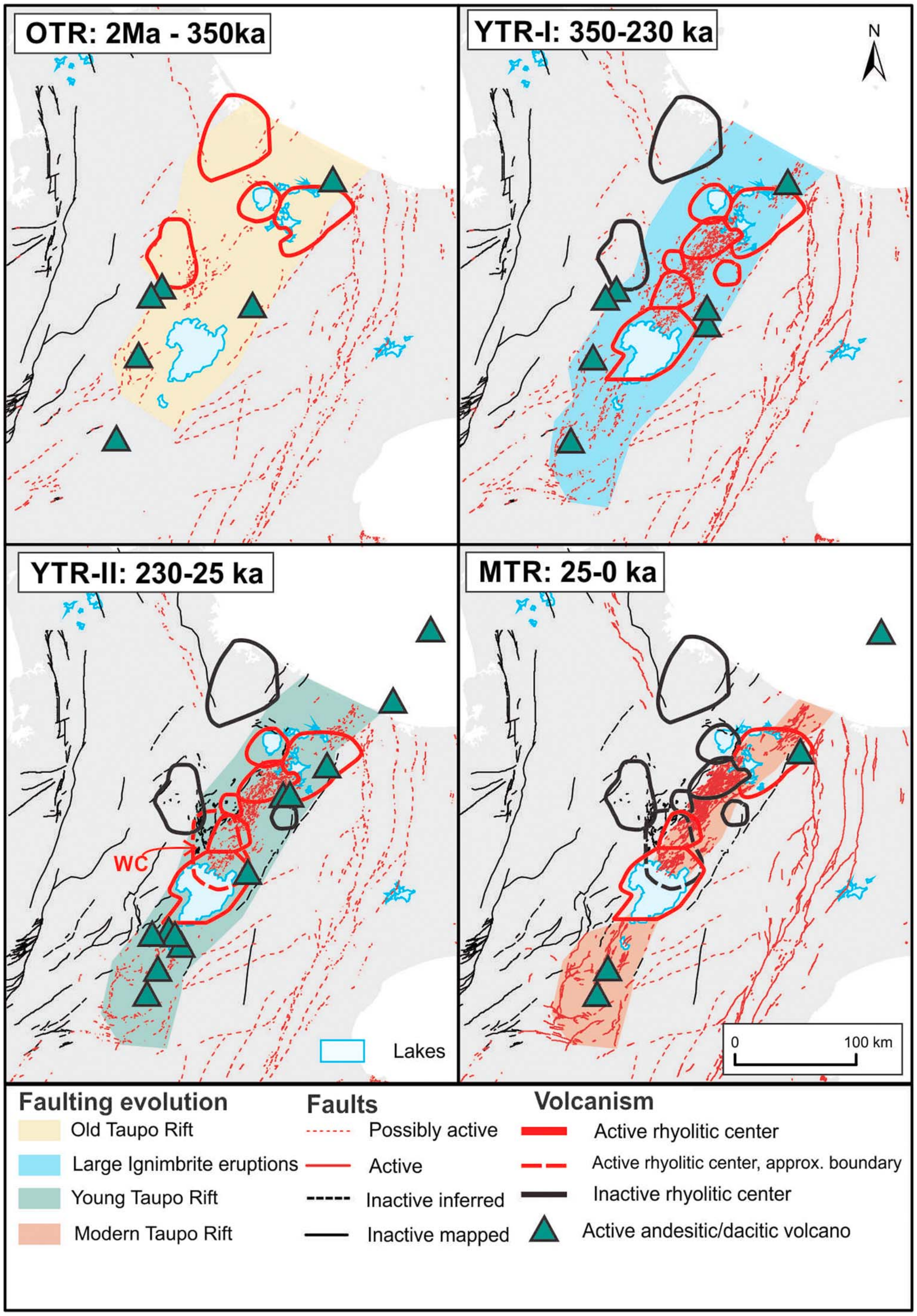

Figure 7. Evolution of active faulting and its relationship with the temporal and spatial evolution of large rhyolitic volcanic centers. Fault localization and propagation follows spatial and temporal evolution of large-volume rhyolitic volcanic centers. Note that we have added a stage here (YTR-I: 350–230 ka) to highlight the extremely voluminous volcanism at this stage (WC, Whakamaru caldera; boundaries are used to represent rhyolitic center, currently buried). Age of volcanism is from Leonard et al. (2010).

Total rates of fault migration can be estimated from this model. In the center, narrowing occurs at an average rate of 25–33 km/Myr. The rift width has narrowed from 70 to ~20 km wide since ~1.5–2 Ma (faults a to d and b to e; Figure 8). Eastward migration of the rift axis (bold arrows in Figure 8) by 15–30 km also occurred between 1.5–2 Ma and ~25–18 ka (an average rate of 8 to 20 km/Myr). Southward propagation occurred at

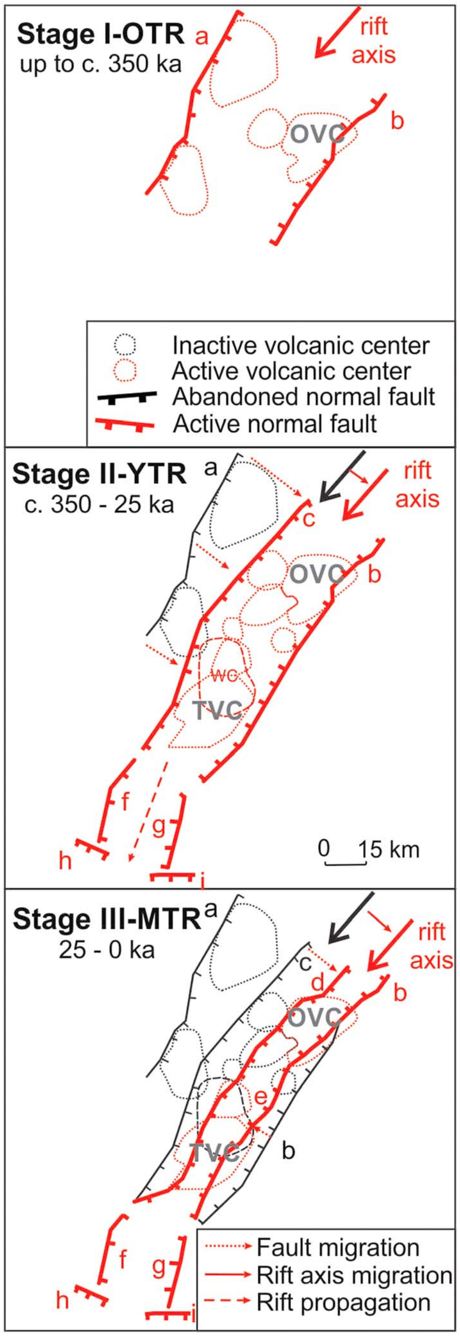

Figure 8. Conceptual model of the modes of fault evolution: inward migration of boundary faults, eastward migration of rift axis, and southward along-strike rift propagation. This sketch displays the location of rift boundary faults at different stages. Stage I or old Taupo Rift (OTR): up to ~350 ka, the Taupo Rift was wider and shorter (a and b are the rift boundary faults). Stage II or young Taupo Rift (YTR): at ~350 to 240 ka, several thousand cubic kilometers of volcanic material erupted from various rhyolitic centers. From 350–240 to 25 ka, the northern and central parts of the rift narrowed with the western boundary (fault a) shifting to the east (to fault c). Also, at this stage the rift started to propagate south (appearance of faults f and g). Stage III or modern Taupo Rift (MTR): from 25 ka to the present, further narrowing of the northern and central parts of the rift occurred (fault c to fault d and fault b to fault e). Migration of the western boundary fault was larger than for the eastern boundary fault resulting in a slight eastward migration of the rift axis.

15–200 km/Myr (to faults f, g, h, and i; i.e., 40 to 70 km in the last ~350 kyr) or ~100–133 km/Myr for the whole rift (from the coast to Ruapehu Volcano) (~200 km in 1.5–2 Ma).

3.2. Processes Controlling the Evolution of the Taupo Rift

In this section we analyze possible processes that may influence the evolution of the Taupo Rift. Our discussion is based on rift processes that have been previously described for other rift settings and/or have been explored using analogue and numerical modeling. We focus our discussion on the three major modes of rift evolution described for the Taupo Rift in Figure 8, namely, width narrowing, lateral migration, and along-strike propagation.

3.2.1. Rift Narrowing (Inward Migration of Faulting)

Narrowing of the Taupo Rift can be explained by both tectonic and magmatic processes. Contributions to rift narrowing from tectonic processes considered here are crustal thinning through extension and the presence of inherited tectonic structures. Progressive tectonic crustal extension with lithospheric necking and thinning has traditionally been regarded as an important contributor to progressive rift narrowing (e.g., England, 1983; Kusznir & Park, 1987; Hopper & Buck, 1996). Initial rift-flanking faults dipping at 60° and cutting through strong, 60 km thick lithosphere create a rift that is approximately 70 km wide (Kissling & Ellis, 2011; Nagel & Buck, 2004; Svartman Dias et al., 2015). To narrow this rift to widths of ~20–30 km by necking requires a total extension of approximately 50–60 km (e.g., Nagel & Buck, 2004; Svartman Dias et al., 2015). However, total extension values for the Taupo Rift are only in the order of ~10 km onshore (Nicol & Wallace, 2007), well short of the ~50 km stretching needed to facilitate narrowing. Also, extension at 1 cm/yr requires larger time intervals of extension (>5 Ma; e.g., Svartman Dias et al., 2015) to narrow the rift than are available in the TVZ. The presence of inherited tectonic structures may facilitate and accelerate rapid narrowing (e.g., Chenin & Beaumont, 2013; Ziegler & Cloetingh, 2004). In the Taupo Rift, the inherited basement structure (Leonard et al., 2010) has a trend subparallel to the rift axis (Seebeck, Nicol, Villamor, et al., 2014), which could aid localization of faulting and enhance rates at which the rift narrowed.

A more important control may be the role of magmatism in narrowing the Taupo Rift, as has been proposed in the evolutionary model above (Figures 7 and 8). The presence of magma within a rift localizes deformation and facilitates extension at lower levels of stress in comparison to purely mechanical faulting or stretching of thick lithosphere (Corti, Bonini, et al., 2003; Buck, 2004). Volcanic centers can act as nuclei for fault localization (e.g., Ellis et al., 2014). Large-scale migration of arc volcanism is mainly controlled by deep-seated processes in the mantle wedge/subduction slab process (England et al., 2004). Therefore, we anticipate that it is more likely that once volcanism is present it will strongly influence fault evolution/migration. Feedback between these two processes in the shallow crust are certainly likely.

The influence of magmatism in rift narrowing has been described for deep and shallow crustal processes. Variations in crustal strength associated with localized volumes of partial melt in the form of deep underplated mafic bodies concentrate stresses and can localize deformation (Buck, 2004; Yamasaki & Gernigons, 2009). Volumes of partial melt or underplating below 10 km in the crust have been described for the central part of the Taupo Rift (Heise et al., 2010) and could have contributed to narrowing of the rift.

Shallow (i.e., $<$10 km) magma chambers can reduce the strength and the effective thickness of the brittle crust creating a weak zone where faulting will localize, facilitating rift narrowing. Extensional deformation of brittle-ductile analogue models, in which locally the brittle layer is thinner because of the presence of a thicker underlying viscous layer, show that normal faulting rapidly localizes above the area of the thinner brittle layer (Corti, Van Wijk, et al., 2003; Corti et al., 2013; Schreurs et al., 2008; Zwaan et al., 2016). As extension occurs and the brittle-ductile transition shallows in the center of the initial graben, faulting migrates inward toward the center of the graben (Corti et al., 2013; Zwaan et al., 2016). The presence of magma bodies will cause the same effect.

Short-term variations in extension and subsidence in the Taupo Rift occur due to contraction and cooling of magma bodies (e.g., Hamling et al., 2016). Over longer time scales, numerical modeling also suggests that magma inflation and weakening in areas undergoing extension can lead to long-term (inelastic) extensional faulting at the edges of the magma body due to stress perturbations (e.g., Ellis et al., 2007, 2011). These effects can persist for thousands to millions of years. Significant narrowing of the Taupo Rift coincides with the extremely large approximately 350–230 ka rhyolite eruptions, suggesting that accumulation of large amounts of rhyolitic magma within the brittle crust at specific locations in a narrow region can promote rift narrowing. Once the rift has narrowed to the width of and at the location of, an active rhyolitic center (in a magmatic segment), adjacent tectonic sections of the rift can narrow through propagation of the new, reduced width along strike. This 3-D effect on propagation has also shown been illustrated by analogue modeling (Schreurs et al., 2008).

Rift narrowing can occur quite rapidly in continental intraarc rifts that form above subduction zones. A probable cause for this fast rate is the presence of crustal heterogeneities related to presence of magmatism from the beginning of rifting; for example, the rift has been superimposed on an active volcanic arc. In contrast, in purely intracontinental settings extension initiates a long time (several millions of years) before the onset of volcanism (e.g., Ebinger, 2005). Once magmatism/volcanism is established and if there is no change in the total extension rate across the graben then rifting evolves faster as the total deformation is localized in a narrower zone. The Taupo Rift is an extreme example; in that, in less than 1.75–1.35 Ma, the rift had substantially narrowed. Rhyolitic supereruptions also create weak zones that disrupt the strength, structure, and stress field of the surrounding crust as large volumes (hundreds of cubic kilometers) are ejected (e.g., Rowland et al., 2010).

3.2.2. Lateral Migration

Lateral rift axis migration can be associated with slab rollback, similar to cross-arc migration of volcanism (e.g., Yamaji, 2003). Worldwide, the location of most active volcanic arcs occurs approximately above the 100 km contour of the subducted slab (England et al., 2004). Eastward migration of older volcanic arcs across of the North Island to the current location (modern TVZ) has been explained by slab rollback (Stern et al., 2006; Seebeck, Nicol, Giba, et al., 2014). Also, eastward migration of back arc rifting in the Lau Basin has been explained by the same phenomenon and displays similar rates (8 to 20 km/Ma; Ruellan et al., 2003, and references therein). Wright et al. (1996) also suggest that the Havre Trough displays cross-arc migration of volcanism, possibly reflecting rollback.

Since the inception of the Taupo Rift, eastward migration has been expressed as a lateral shift of the rift axis, as faulting has always been constrained within the old rift boundaries. It is important to note that given the lack of subsurface information, in particular, for the western part of the rift, we assume a single graben structure for the old rift and assign the axis to the centerline. It is possible that the old rift may have consisted of two or more parallel grabens driven by the presence of several widespread large rhyolitic centers (each of them localizing deformation). Some of the current geological models of geothermal reservoirs suggest the presence of narrow, fault-controlled buried basins (e.g., Chambefort et al., 2014; Downs et al., 2014). These areas could represent locations of graben axes in a prior structural configuration.

3.2.3. Along-Strike Propagation

The mechanism and mode of southward propagation of the onshore Taupo Rift can be explained by either (a) southward migration of the plate boundary forces that are driving the extension, or (b) by large stress perturbations related to large eruptions, or (c) a combination of both. Wallace et al. (2004) propose that the northward increase in extension rates along the Taupo Rift is a consequence of rapid fore-arc block rotations. These rotations result from a combination of the transition from subduction of normal oceanic crust at the Kermadec Trench to subduction of the Hikurangi Plateau at the Hikurangi Trough, and impingement of the Chatham Rise further south, which acts as a pinning point for the southern termination of Hikurangi subduction. Hikurangi subduction is also migrating southward relative to the Australian plate (at 28–37 km/Myr) due to southward migration of the Chatham Rise pinning point relative to Australia. This migration is thought to lead to southward propagation of the Taupo Rift, as the pole of rotation for Hikurangi fore-arc rotation and the subsequent opening of the rift migrate southwestward (Wallace et al., 2007). Similarly, in the Lau Basin, migration of the Louisville Seamount Chain (at ~128 km/Myr) is responsible for the southward propagation of Lau Basin rifting (at 100 km/Myr; Ruellan et al., 2003).

In the southern sector of the Taupo Rift and based on our model (Figure 8), very recent (post-350 ka) southward propagation rates of ~100–200 km/Myr are much higher than the migration of the Chatham Rise pinning point along the plate boundary (28–37 km/Myr). Villamor and Berryman (2006b) proposed that the episodic southward extension of the Taupo Rift was strongly influenced by volcanism (e.g., the volcanic episode at 350–230 kyr). If that is the case, the propagation of the southern 70 km of the rift could have occurred within an even shorter time frame of 120 kyr (between 350 and 230 ka).

The approximately <350 ka propagation of the southern rift sector was more or less coincident in time with the 350–230 ka period of ignimbrite supereruptions. This is also the same period associated with narrowing of the rift from the old Taupo Rift to the young Taupo Rift (Figures 7 and 8). Rotations in principal stress orientations, associated with the massive ignimbrite eruptions in the Lake Taupo area, may have aided rift propagation (e.g., Ellis et al., 2014). Narrowing of the rift to the north shortly before, or during, these eruptions has also aided propagation through the concentration of stresses at the southern tip of the narrow rift.

A similar effect is also described for the occurrence of silicic volcanism as a precursor for on-land propagation in the Afar Rift (Lahitte et al., 2003). There, segment propagation follows the initiation of silicic volcanism. The shallow weak crustal zones (silicic magma chambers) localize the deformation zone, and effusive eruption along fissures also localizes in the same area.

In the evolution of a section of a rift, it is important to consider if the rift has propagated from an initial narrow rift. In the southern Taupo Rift, the original rift width is narrow (~40 km) most likely because it propagated from an already narrowed rift to the north. The presence of a major boundary between basement terranes at this latitude (Seebeck, Nicol, Villamor, et al., 2014) and coeval axial volcanism could have acted as a weak zone and also localized deformation. The different widths of the rift to the north (~20 km wide) and south (~40 km wide) are a consequence of thicker crust in the southern sector (Reyners et al., 2007).

3.3. Evolution Rates and Evolution Reversal: Comparison of Evolutionary Stages of the Taupo Rift With Other Rifts Worldwide

In this section, we aim to compare the evolutionary stages of the Taupo Rift with other currently active rifts in other subduction zones and in intracontinental settings. To define a common frame for evolutionary stages for different tectonic environments, we focus on those aspects that have been described as leading toward, or facilitating, continental breakup. Based on the well-studied East Africa and Main Ethiopian Rift (MER) evolutionary stages (Agostini et al., 2011; Corti, 2009; Ebinger, 2005; Hayward & Ebinger, 1996) and on some aspects of the evolutionary stages described for the Taupo Rift above, we compile processes that lead to continental breakup in Table 1. The evolutionary stages in Table 1 are based on Ebinger (2005), but we distinguish between tectonic and thermal weakening/volcanic processes as the later plays a different role in different tectonic settings. We have mapped the evolutionary stages of several rifts worldwide in Figure 9.

Three types of "rift segments" (segment definition from Hayward & Ebinger (1996)) can be defined, based on the processes that contribute to extension (Table 1): "tectonic segments," where extension is primarily accommodated by normal faulting (i.e., where magmatism is not playing a major role); "tectono-magmatic segments," where extension is accommodated by both dike intrusion and tectonic faulting; and "magmatic segments," where extension is accommodated uniquely by dike intrusion (surface faulting, if present, is a

Table 1
Evolutionary Stages of Rifting of the Continental Lithosphere

Stage	Tectonism	Thermal weakening/volcanism
1—birth	Incipient mechanical stretching of the lithosphere: - Extensional faulting. - Fault trends influenced by existing crustal weakness initially and influenced by extension direction with time.	Incipient thermal weakening and thermal erosion of the lithosphere and slight shallowing of the brittle-ductile transition. (a) Subduction: active thermal erosion of the mantle lithosphere. Some volcanism present. (b) Continent: Passive upwelling of the mantle asthenosphere–decompression melting, magma at the base of the crust. Some melts may reach the surface along the border faults.
2—adolescence	Substantial mechanical stretching of the lithosphere: - Migration of fault activity. - Strain localization near the rift axis. - Border faults lose activity or die.	Substantial thermal weakening and thermal erosion of the lithosphere; substantial shallowing of the brittle-ductile transition. (a) Subduction: underplating and melting of the crust. Large volumes of magma and volcanism along the rift axis. Volcanism may be dominant is some sections of the rift while other adjacent sections remain tectonic. (b) Continent: asthenosphere rises producing more melting. Large volumes of magma extrude along on rift axial faults. Rift segments are mainly magmatic.
3—maturity	Thinned continental lithosphere separates.	(a and b) Oceanic crust created—asthenosphere upwelling and basaltic magmatism.

response to arrested dike intrusion). These three segment types more or less coincide with stages 1, 2, and 3 of Table 1, respectively. However, tectono-magmatic segments can straddle stages 1 and 3 depending on the relative contribution of extension from tectonic faulting versus magmatism.

Based on the evolutionary model for the Taupo Rift described above, it can be divided into two sections: the central and northern Taupo Rift (C-N Taupo Rift; north of, and including, the Taupo Volcanic Center) and the southern Taupo Rift (south of the Taupo Volcanic Center) (Figures 2 and 3). For the C-N Taupo Rift, extension must have been localized on the boundary faults for some time from 2 Ma to produce large displacements (stage 1; Table 1 and Figure 9) as shown in the gravity anomalies. However, given that large rhyolitic eruptions occurred at 1 Ma, it is possible that the C-N Taupo Rift was already displaying characteristics of stage 2 (i.e., thin crust and dominance of volcanic processes) within 1 Ma or less. It is also possible that extension started at the same time as rhyolitic volcanism initiated, which would suggest that the rift never had a very early stage 1 as defined in Table 1. This is difficult to confirm as most information is buried by subsequent volcanic deposits. With certainty, from ~350 ka, the spatiotemporal association of faulting and large rhyolitic centers suggests middle to late stage 2 evolution. Faulting clearly migrated inward and the crust was likely to have substantially thinned by then in some areas, given the extremely large volume of volcanism that occurred during this period (see discussion of current crustal structure and thinning in Wilson & Rowland (2016)). The current C-N Taupo Rift is also at stage 2 with further inward migration of faulting and crustal thinning. However, if we focus on the smaller rift segments within this section of the rift, extensional processes in some segments can be considered purely magmatic (the two currently active Taupo and Okataina Volcanic Centers are at stage 3), while others are purely tectonic (stage 1) in sections between active volcanic centers (e.g., Seebeck & Nicol, 2009; Rowland et al., 2010; Villamor et al., 2011; Allan et al., 2012).

The southern section of the Taupo Rift, south of the Taupo Volcanic Center, has developed recently with faulting present at least since ~400–350 ka (Villamor & Berryman, 2006b). That section has not undergone substantial narrowing (possible initiation of narrowing was documented by Gómez-Vasconcelos et al. (2016), based on deceleration of the eastern boundary fault for the last ~25 ka) and lacks rhyolitic volcanism. The graben is asymmetric with larger displacements on the active eastern boundary (600 m of dip-slip displacement on the Rangipo Fault; Villamor & Berryman, 2006a; Cassidy et al., 2009), which would suggest that large parts of the extension are accommodated by that boundary fault. The presence of active volcanic vents and faulting aligned along the graben axis suggests that this section is tectono-magmatic. However, recent studies suggest that dike intrusion may only account for a small part of the extension rate (<20%; Gómez-Vasconcelos et al., 2017). The crust has not thinned substantially yet (Reyners et al., 2007). These observations suggest that the southern sector of the Taupo Rift has mixed characteristics of late stage 1 to early stage 2.

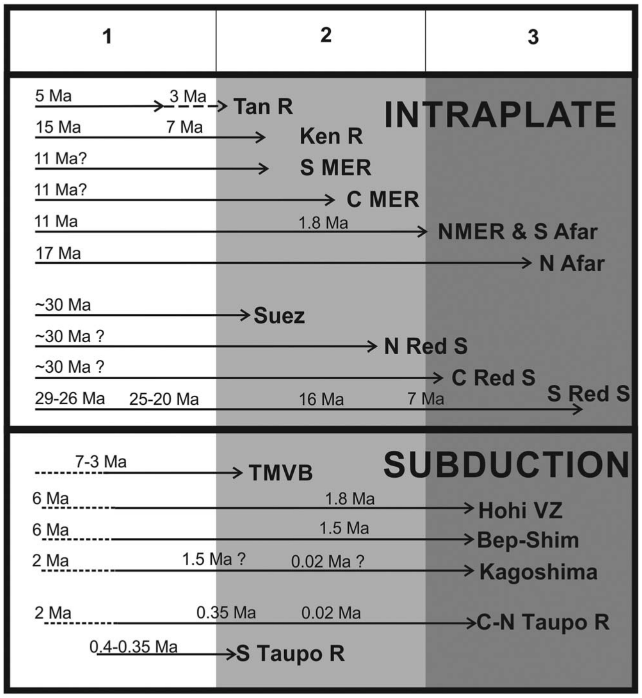

Figure 9. Evolution stages 1 to 3 (see Table 1 for the stage description) for various rifts worldwide: Tan R, Tanzania Rift; Ken R, Kenya Rift; S MER, southern Main Ethiopian Rift; C MER, central Main Ethiopian Rift; N MER, northern Main Ethiopian Rift; S Afar, southern Afar; N Afar, northern Afar; N Red S, northern Red Sea Rift; C Red S, central Red Sea Rift; S Red S, southern Red Sea Rift; TMVB, Trans-Mexican Volcanic Belt; Hohi VZ, Hohi Volcanic Zone; Bep-Shim, Beppu-Shimabara graben; Kagoshima, Kagoshima graben; C-N Taupo R, central and northern Taupo Rift (onshore); S Taupo R, southern Taupo Rift. References consulted for Eastern Africa-MER-Afar system: Hayward and Ebinger (1996), Ebinger (2005), Kendall et al. (2005), Wright et al. (2006), Rowland et al. (2007), Corti (2009), Agostini et al. (2011), and Muirhead et al. (2016). References consulted for Gulf of Suez-Red Sea System: Angelier (1985), Cochran and Martinez (1988), Badawy and Horváth (1999), Bosworth and McClay (2001), Cochran (2005), Wolfenden et al. (2005), Avni et al. (2012), and Abdelwahed et al. (2013). For references on other rifts, see main text.

3.3.1. Evolution of Other Continental Intraarc Rifts in Subduction Zones

Two active continental intraarc rifts, southern Japan and Mexico, have similarities with the Taupo Rift and will be discussed here. From 6 Ma rollback of the West Philippine Basin slab adjacent to the Ryukyu Trench and Kyushu, and rotation of the Kyushu fore arc, has resulted in continental extension (Mahony et al., 2011, and references therein). The two important volcanic rifts in Kyushu, the Beppu-Shimabara graben system (BSGS) and the Kagoshima graben (KG) (Kamata & Kodama, 1999), started at 6 Ma and 2 Ma, respectively. They all currently display evolutionary stages of middle to late stage 2 (Figure 9 and Table 1), based on the thinned crust and the spatial-temporal relationships between volcanism and normal faulting.

Important volcanism, with peaks at 5–4 Ma in the north and 1.5 Ma in the south of BSGS, and at 22–7 ka in the KG (Aramaki, 1984; Kamata, 1989; Yokose et al., 1999; Maeno & Taniguchi, 2007; Mahony et al., 2011), has resulted in areas of thin crust (low seismic velocity zones at ~5 km depth (Saiga et al., 2010); gravity anomalies (Kamata & Kodama, 1994)). The Hohi Volcanic Zone within the Beppu-Shimabara system has undergone clear inward migration of volcanism and faulting (Kamata & Kodama, 1994). Other rifts in Kyushu have no documented fault migration.

Except for the Hohi Volcanic Zone with mainly basaltic volcanism, the Kyushu rifts have important similarities with the Taupo Rift in terms of type of volcanism and the spatial relationships between volcanic centers and faults. Rifts in Kyushu have major rhyolitic centers located in the axial parts of the graben (Yokoyama & Ohkawa, 1986; Hoshizumi et al., 1999). Faults aligned with vents are either in close proximity to the volcanoes or in the sections in between large volcanic centers (https://gbank.gsj.jp/activefault/index_e_gmap.html; Yokoyama & Ohkawa, 1986). This configuration suggests that rifting is accommodated by dike intrusion and faulting in areas around the volcanoes, while in other rift segments extension must be fully accommodated by tectonic faulting (e.g., offshore Shimabara graben is tectonic; Itoh et al., 1998). Additional evidence for coeval contribution to extension from magmatic and tectonic sources is the mismatch between large geodetic extension rates, which should be representative of total extension (Wallace et al., 2009), and geological rates from fault activity, representing only tectonic extension (e.g., 7 versus <3 mm/yr, respectively, in the KG; https://gbank.gsj.jp/activefault/index_e_gmap.html).

One important difference between the BSGS and the Taupo Rift is the angle between rift trend and the basement structural trend (inherited structure). Grabens within the BSGS trend obliquely to the main basement terrain (~40°; Taira, 2001), while the Taupo Rift is subparallel to major basement terrain boundaries (see above). This difference could be responsible for the slightly faster rift evolution in the Taupo Rift.

Extensional faulting (E-W trending) associated with the active Trans-Mexican Volcanic Belt (TMVB) started during a phase of silicic volcanism between 7.5 and 3 Ma, after a pulse of mafic volcanism (which peaked at 11 Ma) that extended from west to east reaching the Gulf of Mexico (Ferrari et al., 2012). The current rift is at a late stage 1 (based on observations from Acambay graben; Figure 9 and Table 1). Most of the deformation is still accommodated by the rift-bounding faults, compared to faults at the graben axis (e.g., Langridge et al., 2000, 2013; Suter et al., 2001; Ortuño et al., 2015), and the crust is still thick (40–50 km) (Suhardja et al., 2015; Urrutia-Fucugauchi & Flores-Ruiz, 1996). However, coeval volcanism and faulting in the graben axis (Sunye-Puchol et al., 2015; Suter et al., 2001) suggests that extension is also partially accommodated by dike intrusion, indicating that the rift is evolving toward stage 2.

The TMVB has strong similarities with the southern Taupo Rift. Active volcanism is somewhat similar in both settings (dominated by dacitic and andesitic stratovolcanoes) and both have thick crust. However, the TMVB seems to be evolving at a slower rate (Figure 9). Causes for a slower evolution are the following: (1) total extension rates are lower in the TMVB (<1 mm/yr, compared to 3–7 mm/yr in the southern Taupo Rift) (Gómez-Vasconcelos et al., 2017; Suter et al., 2001; Villamor & Berryman, 2006a); (2) a somewhat larger initial crustal thickness (it reaches up to 50 km in the eastern sector, compared to 40 km in the southern Taupo Rift); and (3) similar to Kyushu, the basement structure (bedrock structural trends) (e.g., Padilla y Sánchez et al., 2013) in Mexico is very oblique to the rift trend (~70°), making fault localization through inherited structures difficult. An important difference is that the TMVB underwent a period of large ignimbritic eruptions (7–3 Ma) while the southern TVZ has not.

Continental intraarc rifting has also been described for now-extinct rifts (e.g., Busby, 2012). Comparisons with nonactive continental intraarc rifts are beyond the scope of this study. However, we do draw attention to the literature, noting that there are characteristics in the geological record from now-extinct rifts that, for example, record supereruptions, and thick fault-bounded volcano-clastic sequences indicating similar processes and evolutionary patterns to those described here.

3.3.2. Evolution of Intracontinental Rifts

Two well-known active intracontinent rifts, the Eastern Africa (Tanzania, Kenya)-MER (Main Ethiopian Rift)-Afar rift system and the Red Sea-Gulf of Suez system, both in association with the Afar mantle plume, have been described as evolving from early rifting to seafloor spreading (see references in Figure 9). Figure 9 shows the stages of different sections of these two rift systems based on the stage descriptions of Table 1.

These rifts seem to take >10 million years to evolve from a purely tectonic extensional regime (stage 1) toward a regime where volcanism becomes dominant (middle or advanced stage 2) (e.g., Wolfenden et al., 2005) (Figure 9). Studies in younger parts of these rifts suggest that migration of deformation to the axial part may take place as early as 5 to 7 Ma after rift initiation (Ebinger, 2005; Muirhead et al., 2016). Once volcanism and extension have thinned the crust enough and the contribution of magmatic extension supersedes that of tectonic extension (advanced stage 2), the rift may evolve faster toward continental breakup (~2 Ma).

In comparison, the Taupo Rift seems to have evolved rapidly from the beginning, because shallow volcanism is present at early stages. The dominant role of boundary faults in the early stages of intracontinental rifts can be very long lived (e.g., Avni et al., 2012; Bosworth & McClay, 2001) but is short lived in continental subduction rifts (this study).

3.3.3. Evolution Reversal

While most of the settings described above seem to display similar evolution trends, evolution rates vary greatly. Evolution rates are relatively high in rifts associated with subduction zones compared to other environments (<5 Ma to achieve stage 2; Figure 9). In intracontinental settings, the evolution of rifting takes more time, in particular, for the early stages (at least 5 Ma to achieve a late stage 1 and 10+ Ma to achieve a middle stage 2 to early 3; Figure 9) (Ebinger, 2005). In intracontinental rifts, rapid evolution may occur once the crust has sufficiently thinned through thermal weakening (shallow magmatism; e.g., NMER and S Afar seem to have evolved faster in the last ~2 Ma with transitions from middle stage 2 to early stage 3; Figure 9). In continental intraarc rifts, shallow magmatism tends to occur at, or close to, rift initiation.

The study of the evolution of the Taupo Rift provides some additional insights into rift evolution, particularly for the presence of "evolution reversals." There are several segments of the Taupo Rift that were magmatic in the past (or at least tectono-magmatic) that are now purely tectonic. For example, in the area between the Taupo Volcanic Center and the Maroa Volcanic Center to the north (Figure 2), volcanism was dominant ~350–230 kyr ago (Leonard, 2003) and volcanism and dike intrusions have been identified in association with the most recent 25 ka eruption (Allan et al., 2012). However, post-25 ka extension is mainly accommodated by active faulting (e.g., Rowland & Sibson, 2001; Seebeck, Nicol, Villamor, et al., 2014). This suggests that the Maroa area achieved a late evolutionary stage 2 in the past but is now at late stage 1. If we consider the whole sector from the northern coast to Taupo Volcanic Center, it has achieved late stage 2 evolution, but some segments have transitioned from tectonic to magmatic and then reversed.

These fast and recent reversals in evolutionary stages are responsible for contrasting scientific interpretations of the processes controlling extension at specific sites along the Taupo Rift. For example, Wilson and Rowland (2016) discussed, in their view, nonreconciled interpretations by different authors on intrusion versus tectonic derived extension at some sites along the Taupo Rift (e.g., example above on the process at Maroa Volcanic Center at ~25 ka). Most of these controversies disappear as the contrasting interpretations apply to different evolutionary stages of a particular rift segment and mostly to cases where evolution reversals have occurred quite recently.

The presence of evolution reversal is likely to be more common in continental intraarc rifts than in intraplate rifts. The location of volcanism in the shallower parts of the upper crust in intraplate rifts is usually related to the thinning of the brittle crust as a consequence of tectonic extension and/or the location of faulting (e.g., Ebinger, 2005; Keir et al., 2015). In such settings, it seems that once there is a path for the magma to reach the surface that path is further maintained by ongoing extension. However, in subduction zones the location of volcanism is mostly controlled by subduction zone processes. For example, the subduction of oceanic ridges can control the onset and extinction of volcanic activity in the upper crust immediately above the subducted ridge (e.g., the subduction of the Kyushu-Palau ridge led to voluminous volcanism that migrates with the migration of the Philippine Sea Plate; Mahony et al., 2011).

While rapid spatial and temporal variabilities of volcanism in continental intraarc rifts may lead to fast evolution, they may also lead to rapid cessation of extension and rift failure. Other external processes may be necessary to assist breakup such as changes in plate tectonic kinematics (e.g., Bonini et al., 2005) or arrival of a spreading ridge propagator from oceanic into continental crust (similar to the process observed in the Woodlark Rift; Taylor et al., 1995). In the case of the Taupo Rift, the southward propagation of the Lau Rift (Ruellan et al., 2003) into the New Zealand continental margin may facilitate continental breakup.

4. Conclusions

We have presented an evolutionary model of the Taupo Rift in which the rift has narrowed (inward migration of faulting), shifted laterally (lateral migration of the rift axis within the boundaries of the rift), and propagated along strike within the last approximately 2 million years. The evolution model is divided into three stages: the old Taupo Rift from 2 Ma to 350,000 years; the young Taupo Rift from 350,000 years to 25,000 years; and the modern Taupo Rift from 25,000 years to the present. This evolution has occurred at relatively high rates of ~25–33 km/Myr (narrowing; 50 km in 1.5–2 Myr), ~8–20 km/Myr (for eastward migration of the rift axis; 15–30 km in 1.2–1.8 Myr), and ~100–200 km/Myr (southward propagation; 200 km in 2 Myr or 70 km in 350 kyr).

We have described several processes that influence the three stages of evolution and their rate of evolution in subduction-related rifts. For the Taupo Rift we conclude that the presence of shallow large-scale magmatism localizes faulting and once deformation is localized at the rhyolitic center (deformation here is expressed as extension related to dike intrusion), then a new, narrower, rift propagates along strike into nonmagmatic segments of the rift. The subtle eastward shift of the rift axis is mainly controlled by rollback of the subducting slab, and the southward propagation of the rift is linked to southward migration (relative to the Australian Plate) of the Hikurangi Plateau/Chatham Rise subduction pinning point. Correlation in time between a propagation episode, substantial narrowing, and large rhyolite eruptions suggests that voluminous magmatism is aiding along-strike episodic propagation.

We have compared the evolutionary stages of the Taupo Rift with other rifts worldwide. The C-N Taupo Rift is at an evolutionary stage similar to Kyushu, North Red Sea, and central MER rifts. The southern Taupo Rift compares with the Trans-Mexican Volcanic Belt, Suez, and South MER rifts. However, the Taupo Rift achieved mature rift stages faster than the other rifts.

We propose that continental intraarc rifts evolve faster than intraplate rifts. In particular, thinning of the crust and narrowing of the rift is aided by the presence of large heterogeneities in the crust associated with voluminous shallow magmatism. Comparison with other subduction zone settings suggests that the Taupo Rift may have evolved faster than similar continental intraarc rifts in Kyushu and Mexico. Important differences are the trends of inherited basement structure and the rift are almost coincident in the Taupo Rift, while structural trends are quite oblique in the other two rifts; also, extension rates are much larger in Taupo than in Mexico (~3–7; cf. <1 mm/yr).

The overarching rifting processes and stages described here seem to be applicable to different tectonic environments. However, the detailed processes and evolution of early stages may be somewhat more variable in continental intraarc rifts where some segments seem to occasionally revert to less evolved stages. This "evolution reversal" may be a characteristic of continental intraarc rifts, as there is a great spatial and temporal variability in magma supply from the subduction zone. These fast changes may also lead to rift cessation and thus failure to breakup.

Acknowledgments
Financial support came from NZ government funds (GNS Science SSIF), the New Zealand Royal Society Mobility Funds, and Swiss National Fund (SNF 200020-109320 and 200020-122143/1). The authors thank Phaedra Upton, Andy Nicol, Sarah Milicich, Associate Editor and journal referees, Cathy Busby, and Roger Briggs for their reviews of earlier versions of this manuscript. Vaughan Stagpoole provided the residual gravity anomaly map in the supporting information. We wish to especially acknowledge Ian Nairn, who, prior to his retirement, has been an integral part of the research reported here. We dedicate this manuscript to Ian and his many decades of insightful research in the Taupo Rift.

References

Abdelwahed, M. F., El-Khrepy, S., & Qaddah, A. (2013). Three-dimensional structure of Conrad and Moho discontinuities in Egypt. *Journal of the African Earth Sciences*, *85*, 87–102.

Acocella, V., Spinks, K., Cole, J., & Nicol, A. (2003). Oblique back arc rifting of Taupo Volcanic Zone, New Zealand, *Tectonics*, *22*(4), 1045. doi: https://doi.org/10.1029/2002TC001447

Agostini, A., Bonini, M., Corti, G., Sani, F., & Manetti, P. (2011). Distribution of Quaternary deformation in the central Main Ethiopian Rift, East Africa. *Tectonics*, *30*, TC4010. https://doi.org/10.1029/2010TC002833

Allan, A. S., Wilson, C. J. N., Millet, M. A., & Wysoczanski, R. J. (2012). The invisible hand: Tectonic triggering and modulation of a rhyolitic supereruption. *Geology*, *40*(6), 563–566.

Angelier, J. (1985). Extension and rifting: The Zeit region, Gulf of Suez. *Journal of Structural Geology*, *7*(5), 605–612.

Aramaki, S. (1984). Formation of the Aira caldera, southern Kyushu, 22,000 years ago. *Journal of Geophysical Research*, *89*, 8485–8501. https://doi.org/10.1029/JB089iB10p08485

Arehart, G. B., Christenson, B. W., Wood, C. P., Foland, K. A., & Browne, P. R. L. (2002). Timing of volcanic, plutonic and geothermal activity at Ngatamariki, New Zealand. *Journal of Volcanology and Geothermal Research*, *116*(3-4), 201–214.

Avni, Y., Segev, A., & Ginat, H. (2012). Oligocene regional denudation of the northern Afar dome: Pre-and syn-breakup stages of the Afro-Arabian plate. *Geological Society of America Bulletin*, *124*(11-12), 1871–1897.

Badawy, A., & Horváth, F. (1999). The Sinai subplate and tectonic evolution of the northern Red Sea region. *Journal of Geodynamics*, *27*(4), 433–450.

Bannister, S., Bourguignon, S., Sherburn, S., & Bertrand, E. A. (2015). 3-D seismic velocity and attenuation in the central Taupo Volcanic Zone, New Zealand: Imaging the roots of geothermal systems. In Proceedings World Geothermal Congress 2015, Melbourne, Australia, 19–25 April 2015.

Bannister, S., Bryan, C. J., & Bibby, H. M. (2004). Shear wave velocity variation across the Taupo Volcanic Zone, New Zealand, from receiver function inversion. *Geophysical Journal International*, *159*(1), 291–310.

Bannister, S. C., Bourguignon, S., Sherburn, S., & Bertrand, E. A. (2013). Seismic imaging of the central Taupo Volcanic Zone using double-difference tomography. In 35th New Zealand Geothermal Workshop proceedings, 17–20 November 2013, Rotorua, New Zealand.

Beanland, S., Berryman, K. R., & Blick, G. H. (1989). Geological investigations of the 1987 Edgecumbe earthquake, New Zealand. *New Zealand Journal of Geology and Geophysics*, *32*, 73–91.

Begg, J. G., & Mouslopoulou, V. (2010). Analysis of late Holocene faulting within an active rift using lidar, Taupo Rift, New Zealand. *Journal of Volcanology and Geothermal Research*, *190*(1/2), 152–167. https://doi.org/10.1016/j.jvolgeores.2009.06.001

Bibby, H. M., Caldwell, T. G., Davey, F. J., & Webb, T. H. (1995). Geophysical evidence on the structure of the Taupo Volcanic Zone and its hydrothermal circulation. *Journal of Volcanology and Geothermal Research*, *68*(1–3), 29–58.

Bibby, H. M., Risk, G. F., Caldwell, T. G., Heise, W., & Bennie, S. L. (2008). Resistivity structure of western Taupo Volcanic Zone, New Zealand. *New Zealand Journal of Geology and Geophysics*, *51*(3), 231–244.

Blank, H. R. (1965). Ash-flow deposits of the central King Country, New Zealand. *New Zealand Journal of Geology and Geophysics*, *8*(4), 588–607.

Bonini, M., Corti, G., Innocenti, F., Manetti, P., Mazzarini, F., Abebe, T., & Pecskay, Z. (2005). Evolution of the Main Ethiopian Rift in the frame of Afar and Kenya rifts propagation. *Tectonics*, *24*, TC1007. https://doi.org/10.1029/2004TC001680

Bosworth, W., & McClay, K. (2001). Structural and stratigraphic evolution of the Gulf of Suez rift, Egypt: A synthesis. *Mémoires du Muséum National d'Histoire Naturelle*, *186*, 567–606.

Briggs, R. M., Houghton, B. F., McWilliams, M., & Wilson, C. J. N. (2005). $^{40}Ar/^{39}Ar$ ages of silicic volcanic rocks in the Tauranga-Kaimai area, New Zealand: Dating the transition between volcanism in the Coromandel Arc and the Taupo Volcanic Zone. *New Zealand Journal of Geology and Geophysics*, *48*, 459–469.

Briggs, R. M., Lowe, D. J., Esler, W. R., Smith, R. T., Henry, M. A. C., Wehrmann, H., & Manning, D. A. (2006). Geology of the Maketu Area, Bay of Plenty, North Island, New Zealand. In *Occasional Report, 26* (sheet v14, scale 1:50,000, pp. 43). Department of Earth and Ocean Sciences, University of Waikato.

Bryan, C. J., Sherburn, S., Bibby, H. M., Bannister, S. C., & Hurst, A. W. (1999). Shallow seismicity of the central Taupo Volcanic Zone, New Zealand: Its distribution and nature. *New Zealand Journal of Geology and Geophysics*, *42*, 533–542.

Buck, W. R. (2004). Consequences of asthenospheric variability on continental rifting. In G. D. Karner, et al. (Eds.), *Rheology and deformation of the lithosphere at continental margins*, *Theoretical and Experimental Earth Science Series* (Vol. 62, pp. 1–30). New York: Columbia University Press MARGINS.

Busby, C. J. (2012). Extensional and transtensional continental arc basins: Case studies from the southwestern United States. *Tectonics of Sedimentary Basins: Recent Advances*, 382–404.

Cassidy, J., Ingham, M., Locke, C. A., & Bibby, H. (2009). Subsurface structure across the axis of the Tongariro Volcanic Centre, New Zealand. *Journal of Volcanology and Geothermal Research*, *179*(3), 233–240.

Chambefort, I., Lewis, B., Wilson, C. J. N., Rae, A. J., Coutts, C., Bignall, G., & Ireland, T. R. (2014). Stratigraphy and structure of the Ngatamariki geothermal system from new zircon U–Pb geochronology: Implications for Taupo Volcanic Zone evolution. *Journal of Volcanology and Geothermal Research*, *274*, 51–70.

Chenin, P., & Beaumont, C. (2013). Influence of offset weak zones on the development of rift basins: Activation and abandonment during continental extension and breakup. *Journal of Geophysical Research*, *118*, 1698–1720. https://doi.org/10.1002/jgrb.50138

Cochran, J. R., & Martinez, F. (1988). Evidence from the northern Red Sea on the transition from continental to oceanic rifting. *Tectonophysics*, *153*(1–4), 25–53.

Cochran, J. R. (2005). Northern Red Sea: Nucleation of an oceanic spreading center within a continental rift. *Geochemistry, Geophysics, Geosystems*, *6*, Q03006. https://doi.org/10.1029/2004GC000826

Cole, J. W., & Spinks, K. D. (2012). Caldera volcanism and rift structure in the Taupo Volcanic Zone, New Zealand. *Geological Society of London, Special Publication*, *327*, 9–29. https://doi.org/10.1144/SP327.2

Corti, G. (2009). Continental rift evolution: From rift initiation to incipient break-up in the Main Ethiopian Rift, East Africa. *Earth-Science Reviews*, *96*(1), 1–53.

Corti, G., Bonini, M., Conticelli, S., Innocenti, F., Manetti, P., & Sokoutis, D. (2003). Analogue modelling of continental extension: A review focused on the relations between the patterns of deformation and the presence of magma. *Earth-Science Reviews*, *63*, 169–247. https://doi.org/10.1016/S0012-8252(03)00035-7

Corti, G., Ranalli, G., Agostini, A., & Sokoutis, D. (2013). Inward migration of faulting during continental rifting: Effects of pre-existing lithospheric structure and extension rate. *Tectonophysics*, *594*, 137–148.

Corti, G., Van Wijk, J., Bonini, M., Sokoutis, D., Cloetingh, S., Innocenti, F., & Manetti, P. (2003). Transition from continental break-up to punctiform seafloor spreading: How fast, symmetric and magmatic, *Geophysical Research Letters*, *30*(12), 1604. https://doi.org/10.1029/2003GL017374

Downs, D. T., Rowland, J. V., Wilson, C. J. N., Rosenberg, M. D., Leonard, G. S., & Calvert, A. T. (2014). Evolution of the intra-arc Taupo-Reporoa Basin within the Taupo Volcanic Zone of New Zealand. *Geosphere*, *10*(1), 185–206.

Ebinger, C. (2005). Continental break-up: The East African perspective. *Astronomy and Geophysics*, *46*(2), 2–16.

Ebinger, C. J., Yemane, T., Harding, D. J., Tesfaye, S., Kelley, S., & Rex, D. C. (2000). Rift deflection, migration, and propagation: Linkage of the Ethiopian and Eastern rifts, Africa. *Geological Society of America Bulletin*, *112*(2), 163–176.

Ellis, S. M., Heise, W., Kissling, W., Villamor, P., & Schreurs, G. (2014). The effect of crustal melt on rift dynamics: Case study of the Taupo Volcanic Zone. *New Zealand Journal of Geology and Geophysics*, *57*(4), 453–458. https://doi.org/10.1080/00288306.2014.972961

Ellis, S. M., Little, T., Wallace, L. M., Hacker, B. R., & Buiter, S. J. H. (2011). Feedback between rifting and diapirism can exhume ultrahigh-pressure rocks. *Earth and Planetary Science Letters*, *311*, 427–438. https://doi.org/10.1016/j.epsl.2011.09.031

Ellis, S. M., Wilson, C. J. N., Bannister, S., Bibby, H. M., Heise, W., Wallace, L., & Patterson, N. (2007). A future magma inflation event under the rhyolitic Taupo volcano, New Zealand: Numerical models based on constraints from geochemical, geological, and geophysical data. *Journal of Volcanology and Geothermal Research*, *168*, 1–27.

England, P., Engdahl, R., & Thatcher, W. (2004). Systematic variation in the depths of slabs beneath arc volcanoes. *Geophysical Journal International*, *156*, 377–408.

England, P. C. (1983). Constraints on extension of continental lithosphere. *Journal of Geophysical Research*, *88*, 1145–1152. https://doi.org/10.1029/JB088iB02p01145

Ferrari, L., Orozco-Esquivel, T., Manea, V., & Manea, M. (2012). The dynamic history of the Trans-Mexican Volcanic Belt and the Mexico subduction zone. *Tectonophysics*, *522*, 122–149.

Gamble, J. A., Price, R. C., Smith, I. E. M., McIntosh, W. C., & Dunbar, N. W. (2003). ^{40}Ar/^{39}Ar geochronology of magmatic activity, magma flux and hazards at Ruapehu Volcano, Taupo Volcanic Zone, New Zealand. *Journal of Volcanology and Geothermal Research*, *120*(3), 271–287.

Gómez-Vasconcelos, M. G., Villamor, P., Cronin, S. J., Procter, J., Kereszturi, G., Palmer, A., … Ashraf, S. (2016). Earthquake history at the eastern boundary of the South Taupo Volcanic Zone, New Zealand. *New Zealand Journal of Geology and Geophysics*, *59*(4), 522–543. https://doi.org/10.1080/00288306.2016.1195757

Gómez-Vasconcelos, M. G., Villamor, P., Cronin, S. J., Procter, J., Palmer, A., Townsend, D., & Leonard, G. (2017). Crustal extension in the Tongariro graben, New Zealand: Insights into volcano-tectonic interactions and active deformation in a young continental rift. *Geological Society of America Bulletin*. https://doi.org/10.1130/B31657.1

Hamling, I. J., Hreinsdóttir, S., Bannister, S., & Palmer, N. (2016). Off-axis magmatism along a subaerial back-arc rift: Observations from the Taupo Volcanic Zone, New Zealand. *Science Advances*, *2*(6), e1600288.

Hardarson, B. S., Fitton, J. G., & Hjartarson, A. (2008). Tertiary volcanism in Iceland. *Jökull*, *58*, 161–178.

Harrison, A. J., & White, R. S. (2004). Crustal structure of the Taupo Volcanic Zone, New Zealand: Stretching and igneous intrusion. *Geophysical Research Letters*, *31*, L13615. https://doi.org/10.1029/2004GL019885

Hayward, N. J., & Ebinger, C. J. (1996). Variations in the along-axis segmentation of the Afar Rift system. *Tectonics*, *15*, 244–257. https://doi.org/10.1029/95TC02292

Heise, W., Caldwell, T. G., Bibby, H. M., & Bennie, S. L. (2010). Three-dimensional electrical resistivity image of magma beneath an active continental rift, Taupo Volcanic Zone, New Zealand. *Geophysical Research Letters*, *37*, L10301. https://doi.org/10.1029/2010GL043110

Hopper, J. R., & Buck, W. R. (1996). The effect of lower crustal flow on continental extension and passive margin formation. *Journal of Geophysical Research*, *101*(B9), 20,175–20,194. https://doi.org/10.1029/96JB01644

Horspool, N. A., Savage, M. K., & Bannister, S. (2006). Implications for intraplate volcanism and back-arc deformation in northwestern New Zealand, from joint inversion of receiver functions and surface waves. *Geophysical Journal International*, *166*(3), 1466–1483. https://doi.org/10.1111/j.1365-246X.2006.03016.x

Hoshizumi, H., Uto, K., & Watanabe, K. (1999). Geology and eruptive history of Unzen volcano, Shimabara peninsula, Kyushu, SW Japan. *Journal of Volcanology and Geothermal Research*, *89*(1), 81–94.

Houghton, B. F., Wilson, C. J. N., McWilliams, M. O., Lanphere, M. A., Weaver, S. D., Briggs, R. R. M., & Pringle, M. S. (1995). Chronology and dynamics of a large silicic magmatic system: Central Taupo Volcanic Zone, New Zealand. *Geology*, *23*(1), 13–16.

Hurst, T., Heise, W., Hreinsdottir, S., & Hamling, I. (2016). Geophysics of the Taupo Volcanic Zone: A review of recent developments. *Geothermics*, *59*, 188–204.

Itoh, Y., Takemura, K., & Kamata, H. (1998). History of basin formation and tectonic evolution at the termination of a large transcurrent fault system: Deformation mode of central Kyushu, Japan. *Tectonophysics*, *284*, 135–150. https://doi.org/10.1016/S0040-1951(97)00167-4

Kamata, H. (1989). Volcanic and structural history of the Hohi volcanic zone, central Kyushu, Japan. *Bulletin of Volcanology*, *51*, 315–332. https://doi.org/10.1007/BF01056894

Kamata, H., & Kodama, K. (1994). Tectonics of an arc-arc junction: An example from Kyushu Island at the junction of the southwest Japan arc and the Ryukyu arc. *Tectonophysics*, *233*, 69–81. https://doi.org/10.1016/0040-1951(94)90220-8

Kamata, H., & Kodama, K. (1999). Volcanic history and tectonics of the southwest Japan arc. *The Island Arc*, *8*, 393–403. https://doi.org/10.1046/j.1440-1738.1999.00241.x

Keir, D., Bastow, I. D., Corti, G., Mazzarini, F., & Rooney, T. O. (2015). The origin of along-rift variations in faulting and magmatism in the Ethiopian Rift. *Tectonics*, *34*, 464–477. https://doi.org/10.1002/2014TC003698

Kendall, J.-M., Stuart, G. W., Ebinger, C. J., Bastow, I. D., & Keir, D. (2005). Magma-assisted rifting in Ethiopia. *Nature*, *433*(7022), 146–148.

Kissling, W. M., & Ellis, S. M. (2011). Modelling of the flow of hydrothermal fluids above an evolving continental rift. Proceedings of 33th NZ Geothermal Workshop, November 2011.

Kusznir, N. J., & Park, R. G. (1987). The extensional strength of continental lithosphere: Its dependence on geothermal gradient, and crustal composition and thickness. In M. P. Coward, J. F. Dewey, & P. L. Hancock (Eds.), *Continental extensional tectonics* (Vol. 28, pp. 35–52). Geological Society London, Special Publication.

Lahitte, P., Gillot, P. Y., & Courtillo, V. (2003). Silicic central volcanoes as precursors to rift propagation: The Afar case. *Earth and Planetary Science Letters*, *207*(1), 103–116.

Lamarche, G., Barnes, P. M., & Bull, J. M. (2006). Faulting and extension rate over the last 20,000 years in the offshore Whakatane graben, New Zealand continental shelf. *Tectonics*, *25*, TC4005. https://doi.org/10.1029/2005TC001886

Langridge, R. M., Persaud, M., Zúñiga, F. R., Aguirre-Díaz, G. J., Villamor, P., & Lacan, P. (2013). Preliminary paleoseismic results from the Pastores fault and its role in the seismic hazard of the Acambay graben, Trans-Mexican Volcanic Belt, Mexico. *Revista Mexicana de Ciencias Geológicas*, *30*(3), 463–481.

Langridge, R. M., Weldon, R. J., Moya, J. C., & Suárez, G. (2000). Paleoseismology of the 1912 Acambay earthquake and the Acambay-Tixmadejé fault, Trans-Mexican volcanic belt. *Journal of Geophysical Research*, *105*(B2), 3019–3037. https://doi.org/10.1029/1999JB900239

Lee, J. M., Townsend, D., Bland, K., & Kamp, P. J. J. (2010). Geology of the Hawke's Bay area, GNS Science, Institute of Geological & Nuclear Sciences Limited, Lower Hutt, New Zealand (map 8, scale 1:250,000, 1 sheet, 86 p.).

Leonard, G. S. (2003). The evolution of Maroa Volcanic Centre, Taupo Volcanic Zone, New Zealand, unpub. (PhD thesis), Christchurch, New Zealand, University of Canterbury, 321 p.

Leonard, G. S., Begg, J. G., & Wilson, C. J. N. (2010). Geology of the Rotorua area: GNS Science, Institute of Geological & Nuclear Sciences Limited, geological (map 5, scale 1:250,000, 1 sheet, 102 p.).

Litchfield, N. J., Van Dissen, R., Sutherland, R., Barnes, P. M., Cox, S. C., Norris, R., … Stirling, M. (2014). A model of active faulting in New Zealand. *New Zealand Journal of Geology and Geophysics*, *57*(1), 32–56.

Maeno, F., & Taniguchi, H. (2007). Spatiotemporal evolution of a marine caldera-forming eruption, generating a low-aspect ratio pyroclastic flow, 7.3 ka, Kikai caldera, Japan: Implication from near-vent eruptive deposits. *Journal of Volcanology and Geothermal Research*, *167*(1), 212–238.

Mahony, S. H., Wallace, L. M., Miyoshi, M., Villamor, P., Sparks, R. S. J., & Hasenaka, T. (2011). Volcano-tectonic interactions during rapid plate-boundary evolution in the Kyushu region, SW Japan. *Geological Society of America Bulletin*, *123*(11-12), 2201–2223.

Manning, D. A. (1995). Late Pleistocene tephrostratigraphy of the Eastern Bay of Plenty Region, New Zealand, unpub. (PhD thesis), Wellington, New Zealand, Victoria University, 321 p.

Manville, V., & Wilson, C. J. N. (2004). The 26.5 ka Oruanui eruption, New Zealand: A review of the roles of volcanism and climate in the post-eruptive sedimentary response. *New Zealand Journal of Geology and Geophysics*, *47*, 525–547.

McNamara, D. D., Sewell, S., Buscarlet, E., & Wallis, I. C. (2016). A review of the Rotokawa geothermal field, New Zealand. *Geothermics*, *59*, 281–293.

Milicich, S. D, M.A. van Dam, M.D. Rosenberg, A.J. Rae, and G. Bignall (2010). "Earth Research" 3-dimensional geological modelling of a geothermal system in New Zealand; a new visualization tool. In Proceedings of the World Geothermal Congress, Bali, Indonesia.

Milicich, S. D., Wilson, C. J. N., Bignall, G., Pezaro, B., & Bardsley, C. (2013). Reconstructing the geological and structural history of an active geothermal field, A case study from New Zealand. *Journal of Volcanology and Geothermal Research*, *262*, 7–24.

Milicich, S. D., Wilson, C. J. N., Bignall, G., Pezaro, B., Charlier, B. L. A., Wooden, J. L., & Ireland, T. R. (2013). U–Pb dating of zircon in hydrothermally altered rocks of the Kawerau Geothermal Field, Taupo Volcanic Zone, New Zealand. *Journal of Volcanology and Geothermal Research*, *253*, 97–113. https://doi.org/10.1016/j.jvolgeores.2012.12.016

Mouslopoulou, V., Nicol, A., Walsh, J. J., Beetham, D., & Stagpoole, V. (2008). Quaternary temporal stability of a regional strike-slip and rift fault intersection. *Journal of Structural Geology*, *30*, 451–463. https://doi.org/10.1016/j.jsg.2007.12.005

Mroczek, E. K., Milicich, S. D., Bixley, P. F., Sepulveda, F., Bertrand, E. A., Soengkono, S., & Rae, A. (2016). Ohaaki geothermal system: Refinement of a conceptual reservoir model. *Geothermics*, *59*, 311–324.

Muirhead, J. D., Kattenhorn, S. A., Lee, H., Mana, S., Turrin, B. D., Fischer, T. P., … Stamps, D. S. (2016). Evolution of upper crustal faulting assisted by magmatic volatile release during early-stage continental rift development in the East African Rift. *Geosphere*, *12*(6), 1670–1700.

Nagel, T. J., & Buck, W. R. (2004). Symmetric alternative to asymmetric rifting models. *Geology*, *32*(11), 937–940.

Nairn, I. A. (2002). Geology of the Okataina Volcanic Center: Institute of Geological & Nuclear Sciences, Lower Hutt, New Zealand, map 25, scale 1:50 000, 1 sheet, 156p text.

Nicol, A., & Wallace, L. M. (2007). Temporal stability of deformation rates: Comparison of geological and geodetic observations, Hikurangi subduction margin, New Zealand. *Earth and Planetary Science Letters*, *258*, 397–413.

Nicol, A., Walsh, J., Mouslopoulou, V., & Villamor, P. (2009). Earthquake histories and Holocene acceleration of fault displacement rates. *Geology*, *37*, 911–914.

Ortuño, M., Zúñiga, F. R., Aguirre-Díaz, G. J., Carreón-Freyre, D., Cerca, M., & Roverato, M. (2015). Holocene paleo-earthquakes recorded at the transfer zone of two major faults: The Pastores and Venta de Bravo faults (Trans-Mexican Volcanic Belt). *Geosphere*, *11*(1), 160–184.

Padilla y Sánchez, R. J., Domínguez Trejo, I., López Azcárraga, A. G., Mota Nieto, J., Fuentes Menes, A. O., Rosique Naranjo, F., Germán Castelán, E. A., & Campos Arriola, S. E. (2013). National Autonomous University of Mexico tectonic map of Mexico GIS Project, *American Association of Petroleum Geologists GIS Open Files series*.

Parson, L. M., & Wright, I. C. (1996). The Lau-Havre-Taupo back-arc basin: A southward propagating, multi-stage evolution from rifting to spreading. *Tectonophysics*, *263*, 1–22. https://doi.org/10.1016/S0040-1951(96)00029-7

Price, R. C., Gamble, J. A., Smith, I. E. M., Stewart, R. B., Eggins, S., & Wright, I. C. (2005). An integrated model for the temporal evolution of andesites and rhyolites and crustal development in New Zealand's North Island. *Journal of Volcanology and Geothermal Research*, *140*(1), 1–24.

Reyners, M., Eberhart-Phillips, D., & Stuart, G. (2007). The role of fluids in lower-crustal earthquakes near continental rifts. *Nature*, *446*(7139), 1075–1078.

Rowland, J. V., Baker, E., Ebinger, C. J., Keir, D., Kidane, T., Biggs, J., … Wright, T. J. (2007). Fault growth at a nascent slow-spreading ridge: 2005 Dabbahu rifting episode, Afar. *Geophysical Journal International*, *171*(3), 1226–1246.

Rowland, J. V., & Sibson, R. H. (2001). Extensional fault kinematics within the Taupo Volcanic Zone, New Zealand: Soft-linked segmentation of a continental rift system. *New Zealand Journal of Geology and Geophysics*, *44*, 271–283.

Rowland, J. V., Wilson, C. J. N., & Gravley, D. M. (2010). Spatial and temporal variations in magma-assisted rifting, Taupo Volcanic Zone, New Zealand. *Journal of Volcanology and Geothermal Research*, *190*(1), 89–108.

Ruellan, E., Delteil, J., Wright, I., & Matsumoto, T. (2003). From rifting to active spreading in the Lau Basin–Havre Trough backarc system (SW Pacific): Locking/unlocking induced by seamount chain subduction. *Geochemistry, Geophysics, Geosystems*, *4*(5), 8909. https://doi.org/10.1029/2001GC000261.

Saiga, A., Matsumoto, S., Uehira, K., Matsushima, T., & Shimizu, H. (2010). Velocity structure in the crust beneath the Kyushu area. *Earth, Planets and Space*, *62*(5), 449.

Schreurs, G., Ellis, S., & Villamor, P. (2008). The southern termination of the Taupo Rift (North Island, New Zealand): Insights from 3D analogue and numerical models. *Bulletin of Geofisica*, *49*, 336–338.

Seebeck, H., & Nicol, A. (2009). Dike intrusion and displacement accumulation at the intersection of the Okataina Volcanic Centre and Paeroa Fault zone, Taupo Rift, New Zealand. *Tectonophysics*, *475*(3), 575–585.

Seebeck, H., Nicol, A., Giba, M., Pettinga, J., & Walsh, J. (2014). Geometry of the subducting Pacific plate since 20 Ma, Hikurangi margin, New Zealand. *Journal of the Geological Society of London*, *171*, 131–143.

Seebeck, H., Nicol, A., Villamor, P., Ristau, J., & Pettinga, J. (2014). Structure and kinematics of the Taupo Rift, New Zealand. *Tectonics*, *33*, 1178–1199. https://doi.org/10.1002/2014TC003569

Sherburn, S., Bannister, S., & Bibby, H. (2003). Seismic velocity structure of the central Taupo Volcanic Zone, New Zealand, from local earthquake tomography. *Journal of Volcanology and Geothermal Research*, *122*(1), 69–88.

Stagpoole, V. M. (1994). Interpretation of refraction seismic and gravity data across the eastern margin of the Taupo Volcanic Zone. *Geothermics*, *23*, 501–510.

Stagpoole, V. M., & Bibby, H. M. (1999). Residual gravity anomaly map of the Taupo Volcanic Zone, New Zealand: Lower Hutt, Institute of Geological & Nuclear Sciences, Institute of Geological & Nuclear Sciences geophysical map 13, 1 map, scale 1:250 000.

Stern, T., & Benson, A. (2011). Wide-angle seismic imaging beneath an andesitic arc: Central North Island, New Zealand. *Journal of Geophysical Research*, *116*, B09308. https://doi.org/10.1029/2011JB008337

Stern, T. A., Stratford, W. R., & Salmon, M. L. (2006). Subduction evolution and mantle dynamics at a continental margin: Central North Island, New Zealand. *Reviews of Geophysics*, *44*, RG4002. https://doi.org/10.1029/2005RG000171

Suhardja, S. K., Grand, S. P., Wilson, D., Guzman-Speziale, M., Gomez-Gonzalez, J. M., Dominguez-Reyes, T., & Ni, J. (2015). Crust and subduction zone structure of southwestern Mexico. *Journal of Geophysical Research: Solid Earth*, *120*, 1020–1035. https://doi.org/10.1002/2014JB011573

Sunye-Puchol, I., Lacan, P., Ortuño, M., Villamor, P., Audin, L., Zuniga, F. R., … Lawton, T. F. (2015). The San Mateo fault: New paleoseismological evidence of active faulting in the Acambay graben, Mexico. *Revista Mexicana Ciencias Geologicas*, *32*(3), 361–376.

Suter, M., López-Martínez, M., Quintero-Legorreta, O., & Carrillo-Martínez, M. (2001). Quaternary intra-arc extension in the central Trans-Mexican volcanic belt. *Geological Society of America Bulletin*, *113*(6), 693–703.

Svartman Dias, A. E., Lavier, L. L., & Hayman, N. W. (2015). Conjugate rifted margins width and asymmetry: The interplay between lithospheric strength and thermomechanical processes. *Journal of Geophysical Research: Solid Earth*, *120*, 8672–8700. https://doi.org/10.1002/2015JB012074

Taira, A. (2001). Tectonic evolution of the Japanese island arc system. *Annual Review of Earth and Planetary Sciences*, *29*, 109–134. https://doi.org/10.1146/annurev.earth.29.1.109

Taylor, B., Goodlife, A., Martinez, F., & Hey, R. (1995). Continental rifting and initial seafloor spreading in Woodlark Basin. *Nature*, *374*, 534–537.

Taylor, S. K., Bull, J. M., Lamarche, G., & Barnes, P. M. (2004). Normal fault growth and linkage during the last 1.3 million years: An example from the Whakatane Graben, New Zealand. *Journal of Geophysical Research*, *109*, B02408. https://doi.org/10.1029/2003JB002412

Townsend, D., Vonk, A., & Kamp, P. J. J. (2008). Geology of the Taranaki area: GNS Science, Institute of Geological & Nuclear Sciences, Lower Hutt, New Zealand, (scale 1:250 000, geological map 7, 1 sheet, 77 p.).

Urrutia-Fucugauchi, J., & Flores-Ruiz, J. H. (1996). Bouguer gravity anomalies and regional crustal structure in central Mexico. *International Geology Review*, *38*, 2176–2194.

Vandergoes, M. J., Hogg, A. G., Lowe, D. J., Newnham, R. M., Denton, G. H., Southon, J., … Blaauw, M. (2013). A revised age for the Kawakawa/Oruanui tephra, a key marker for the Last Glacial Maximum in New Zealand. *Quaternary Science Reviews*, *74*, 195–201. https://doi.org/10.1016/j.quascirev.2012.11.006

Villamor, P., & Berryman, K. R. (2001). A late Quaternary extension rate in the Taupo Volcanic Zone, New Zealand, derived from fault slip data. *New Zealand Journal of Geology and Geophysics*, *44*, 243–269.

Villamor, P., & Berryman, K. R. (2006a). Late Quaternary geometry and kinematics of faults at the southern termination of the Taupo Volcanic Zone, New Zealand. *New Zealand Journal of Geology and Geophysics*, *49*(1), 1–21.

Villamor, P., & Berryman, K. R. (2006b). Evolution of the southern termination of the Taupo Volcanic Zone. *New Zealand Journal of Geology and Geophysics*, *49*(1), 23–27.

Villamor, P., Berryman, K. R., Nairn, I. A., Wilson, K., Litchfield, N. J., & Ries, W. (2011). Associations between volcanic eruptions from Okataina volcanic center and surface rupture of nearby active faults, Taupo Rift, New Zealand, Insights into the nature of volcano-tectonic interactions. *Geological Society of America Bulletin*, *123*(7/8), 1383–1405. https://doi.org/10.1130/B30184.1

Wallace, L. M., Beavan, J., McCaffrey, R., & Darby, D. (2004). Subduction zone coupling and tectonic block rotations in the North Island, New Zealand. *Journal of Geophysical Research*, *109*, B12406. https://doi.org/10.1029/2004JB003241

Wallace, L. M., Beavan, R. J., McCaffrey, R., Berryman, K. R., & Denys, P. (2007). Balancing the plate motion budget in the South Island, New Zealand using GPS, geological and seismological data. *Geophysical Journal International*, *168*(1), 332–352. https://doi.org/10.1111/j.1365-246X.2006.03183.x

Wallace, L. M., Ellis, S., Miyao, K., Miura, S., Beavan, J., & Goto, J. (2009). Enigmatic, highly active left-lateral shear zone in southwest Japan explained by aseismic ridge collision. *Geology*, *37*(2), 143–146.

Wilson, C. J. N., Gravley, D. M., Leonard, G. S., & Rowland, J. V. (2009). Volcanism in the central Taupo Volcanic Zone, New Zealand: Tempo, styles and controls. In *Studies in volcanology: The legacy of George Walker*, *Special Publications of IAVCEI* (Vol. 2, pp. 225–247).

Wilson, C. J. N., Houghton, B. F., McWilliams, M. O., Lanphere, M. A., Weaver, S. D., & Briggs, R. M. (1995). Volcanic and structural evolution of Taupo Volcanic Zone, New Zealand: A review. *Journal of Volcanology and Geothermal Research*, *68*, 1–28.

Wilson, C. J. N., Rhoades, D. A., Lanphere, M. A., Calvert, A. T., Houghton, B. F., Weaver, S. D., & Cole, J. W. (2007). A multiple-approach radiometric age estimate for the Rotoiti and Earthquake Flat eruptions, New Zealand, with implications for the MIS 4/3 boundary. *Quaternary Science Reviews*, *26*(13/14), 1861–1870. https://doi.org/10.1016/j.quascirev.2007.04.017)

Wilson, C. J. N., & Rowland, J. V. (2016). The volcanic, magmatic and tectonic setting of the Taupo Volcanic Zone, New Zealand, reviewed from a geothermal perspective. *Geothermics*, *59*, 168–187.

Wolfenden, E., Ebinger, C., Yirgu, G., Renne, P. R., & Kelley, S. P. (2005). Evolution of a volcanic rifted margin: Southern Red Sea, Ethiopia. *Geological Society of America Bulletin*, *117*(7/8), 846–864. https://doi.org/10.1130/B25516.1

Wright, I. C., Parson, L. M., & Gamble, J. A. (1996). Evolution and interaction of migrating cross-arc volcanism and backarc rifting: An example from the southern Havre Trough (35°20′–37°S). *Journal of Geophysical Research*, *101*(B10), 22,071–22,086. https://doi.org/10.1029/96JB01761

Wright, T. J., Ebinger, C., Biggs, J., Ayele, A., Yirgu, G., Keir, D., & Stork, A. (2006). Magma-maintained rift segmentation at continental rupture in the 2005 Afar dyking episode. *Nature*, *442*(7100), 291–294.

Yamaji, A. (2003). Slab rollback suggested by latest Miocene to Pliocene forearc stress and migration of volcanic front in southern Kyushu, northern Ryukyu arc. *Tectonophysics*, *364*, 9–24.

Yamasaki, T., & Gernigons, L. (2009). Styles of lithospheric extension controlled by underplated mafic bodies. *Tectonophysics*, *468*, 169–184.

Yokose, H., Yanashima, T., Kikuchi, W., Sugiyama, N., Shinohara, A., Takeuchi, T., … Kodama, K. (1999). Episodic magmatism since 5 Ma in the western part of Beppu-Shimabara graben, Kyushu, Japan. *Journal of Mineralogy Petrology and Economic Geology*, *94*, 338–348. https://doi.org/10.2465/ganko.94.338

Yokoyama, I., & Ohkawa, S. (1986). The subsurface structure of the Aira caldera and its vicinity in southern Kyushu, Japan. *Journal of Volcanology and Geothermal Research*, *30*(3-4), 253–282.

Ziegler, P. A., & Cloetingh, S. (2004). Dynamic processes controlling evolution of rifted basins. *Earth-Science Reviews*, *64*, 1–50.

Zwaan, F., Schreurs, G., Naliboff, J., Buiter, S. J., & S. J. (2016). Insights into the effects of oblique extension on continental rift interaction from 3D analogue and numerical models. *Tectonophysics*, *693*, 239–260.